Research Paper

GEOSPHERE

GEOSPHERE, v. 15, no. 4

https://doi.org/10.1130/GES02033.1

15 figures; 1 table; 5 supplemental files

CORRESPONDENCE: geowat@uky.edu

CITATION: Thomas, W.A., Gehrels, G.E., Lawton, T.F., Satterfield, J.I., Romero, M.C., and Sundell, K.E., 2019, Detrital zircons and sediment dispersal from the Coahuila terrane of northern Mexico into the Marathon foreland of the southern Midcontinent: Geosphere, v. 15, no. 4, p. 1102–1127, https://doi.org/10.1130/GES02033.1.

Science Editor: David Fastovsky
Associate Editor: Nancy Riggs

Received 5 July 2018
Revision received 27 February 2019
Accepted 3 May 2019

Published online 26 June 2019

Detrital zircons and sediment dispersal from the Coahuila terrane of northern Mexico into the Marathon foreland of the southern Midcontinent

William A. Thomas[1], George E. Gehrels[2], Timothy F. Lawton[3], Joseph I. Satterfield[4], Mariah C. Romero[5], and Kurt E. Sundell[2]

[1]Emeritus, University of Kentucky, and Geological Survey of Alabama, P.O. Box 869999, Tuscaloosa, Alabama 35486-6999, USA
[2]Department of Geosciences, University of Arizona, Tucson, Arizona 85721, USA
[3]Centro de Geociencias, Universidad Nacional Autónoma de México (UNAM), Juriquilla, Querétaro 76230, Mexico
[4]Department of Physics and Geosciences, Angelo State University, San Angelo, Texas 76909, USA
[5]Department of Earth Sciences, Montana State University, Bozeman, Montana 59717, USA

ABSTRACT

New analyses of U-Pb ages along with previously published analyses of detrital zircons from sandstones in the foreland of the Marathon orogen in west Texas have significant implications regarding provenance. The most prominent concentrations of U-Pb ages are at 1200–1000, 700–500, and 500–290 Ma. The accreted Coahuila terrane in the Marathon hinterland and nearby terranes with Gondwanan (Amazonia) affinity include Paleozoic volcanic and plutonic rocks, as well as Precambrian basement rocks. Late Paleozoic Las Delicias arc rocks have ages of 331–270 Ma. Detrital zircons from Upper Jurassic and Lower Cretaceous sandstones, which were deposited in local basins around the Coahuila terrane, provide a record of detritus available from proximal sources within Coahuila, including important peaks at 1040, 562, 422, 414, 373, and 282 Ma. Components of the detrital-zircon populations in the Marathon foreland have unique matches with primary and/or detrital sources in the Coahuila terrane. Although some components of the Marathon populations also have age matches in Laurentia (Appalachians), others do not; however, all components of the Marathon populations have potential sources in Coahuila. Analyses of εHf_t show generally more negative values in Amazonia than in Laurentia, and εHf_t values for Marathon sandstones have distributions similar to those in Amazonia. Therefore, the Coahuila terrane provides a provenance for all of the detrital-zircon ages in the Marathon foreland, requiring no mixing from other sources.

INTRODUCTION

The late Paleozoic Ouachita-Marathon orogen, along the southern margin of the North American Midcontinent, includes foreland basins, thrust belts, subduction complexes, and accreted terranes (Fig. 1) (Arbenz, 1989; Viele and Thomas, 1989). Thrust propagation incorporated the proximal parts of the fill of the foreland basins, and we use the term "Marathon foreland" to encompass both the distal foreland basin and the proximal foreland basin in the thrust belt. Much of the late Paleozoic orogenic belt is covered by postorogenic strata of the Gulf Coastal Plain; and, as a result, geologic interpretations are based on the relatively extensive exposure in the Ouachita Mountains in Arkansas and Oklahoma and a smaller exposure in the Marathon thrust belt and foreland of west Texas, as well as on drill holes and geophysical data (Thomas et al., 1989). Large-scale cratonward convex curves of the thrust belt define the Marathon and Ouachita salients, which are adaptations to the shapes of the Marathon and Ouachita embayments of the pre-orogenic Laurentian margin (Fig. 1) (Thomas, 1977). The Ouachita-Marathon allochthon consists of Cambrian–Mississippian off-shelf, deep-water, mud-dominated, passive-margin strata and Mississippian–Permian synorogenic clastic wedges, which were thrust over autochthonous Cambrian–Mississippian passive-margin shelf facies and Precambrian continental crust (Viele and Thomas, 1989; Hickman et al., 2009). Along the orogen, foreland basins vary in details of subsidence and filling history (Arbenz, 1989). Terranes of continental crust and continental-margin arcs in the internal parts of the Ouachita-Marathon orogen were accreted along the pre-orogenic lapetan rifted margin of Laurentia (Fig. 1) (Viele and Thomas, 1989). The accreted terranes are well documented by gravity profiles, which indicate full-thickness continental crust in the Coahuila terrane within the Marathon salient of the thrust belt and in the Sabine terrane within the Ouachita salient (Keller et al., 1989a, 1989b; Mickus and Keller, 1992).

Broadly similar successions of thick synorogenic clastic wedges, beginning with muddy turbidites that overlie the chert-dominated upper part of the off-shelf, passive-margin succession, define the Marathon and Ouachita foreland basins, which have large amplitude-to-wavelength ratios (Arbenz, 1989; Viele and Thomas, 1989). The muddy succession grades upward into more-sandy turbidites, which include some boulder beds. Interpretations of sediment provenance and dispersal range from proximal orogenic sources (e.g., Brown, 1973; Ross, 1986; Thompson, *in* Johnson et al., 1988; McBride, 1989) to recycling and dispersal from distant sources in the Appalachian orogen across the craton or along the continental slope and rise to basins at the Ouachita and Marathon continental margin (Graham et al., 1976). Some interpretations include a mixture of proximal orogenic sources and more distally supplied sediment from the Appalachians (e.g., Gleason et al., 2007; Soreghan and Soreghan, 2013).

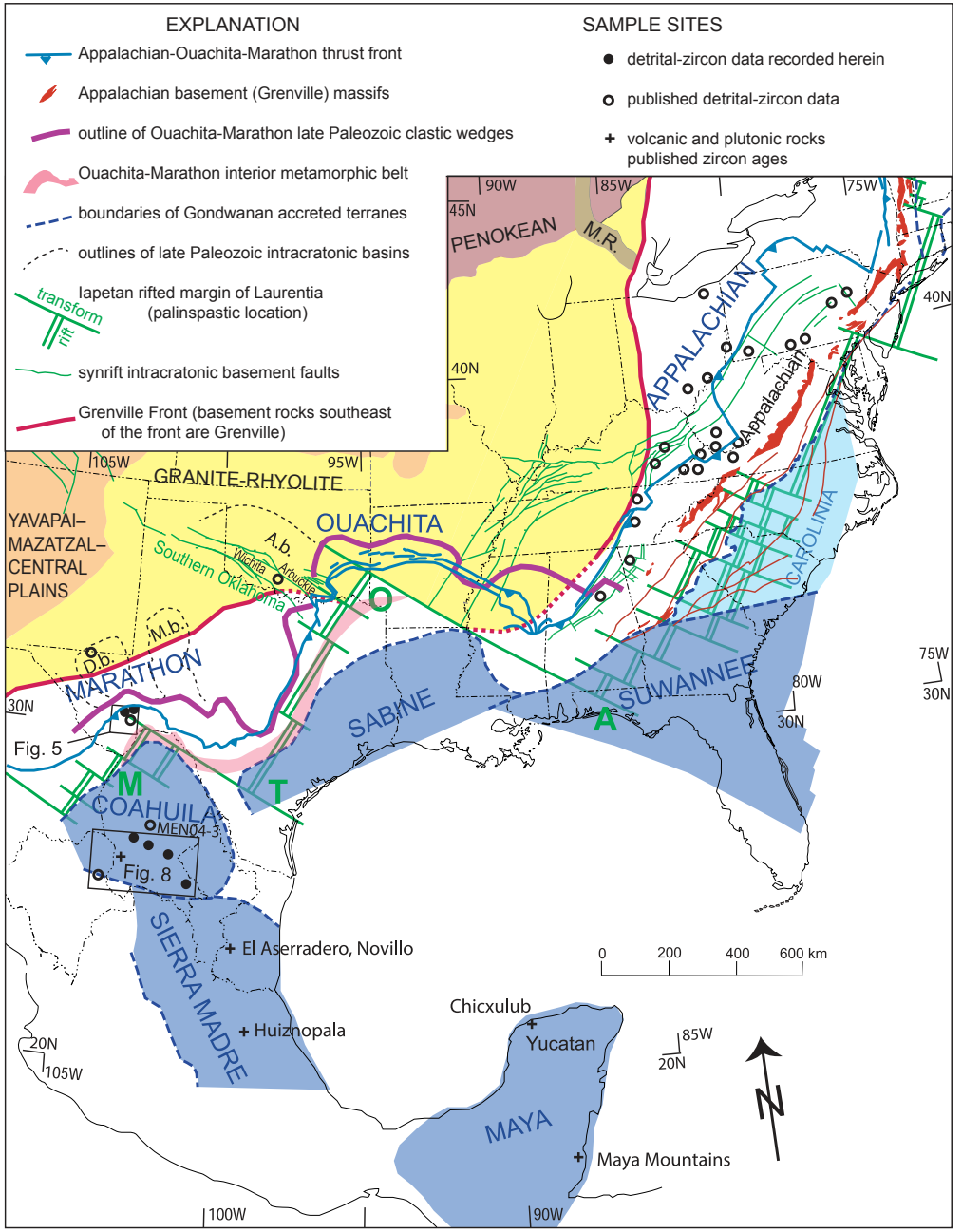

Figure 1. Regional map of the Marathon foreland and related large-scale structural elements: Precambrian provinces (M.R.—Midcontinent rift) of the craton (modified from Van Schmus et al., 1993); lapetan rift margin and synrift intracratonic faults of Laurentia (multiple parallel rift symbols represent lower-plate extension), which outline the locations of synrift igneous and sedimentary rocks, as well as the approximate trace of the passive-margin shelf edge (from Thomas, 2014); locations of Gondwanan accreted terranes (from Krogh et al., 1993; Steiner and Walker, 1996; Stewart et al., 1999; Dickinson and Lawton, 2001; Centeno-García, 2005; Poole et al., 2005; Hibbard et al., 2007; Hatcher, 2010; Martens et al., 2010; Thomas, 2014); trace of the Appalachian-Ouachita thrust front and Ouachita interior metamorphic belt (compiled from Thomas et al., 1989, and Hatcher, 2010); Appalachian basement massifs of Grenville-age rocks (Hatcher, 2010); and outline of late Paleozoic clastic wedges along the Ouachita orogen (from Thomas, 2006). Promontories and embayments of Iapetan rifted margin of Laurentia (green type): A—Alabama promontory; O—Ouachita embayment; T—Texas promontory; M—Marathon embayment. Late Paleozoic intracratonic basins (black type): A.b.—Anadarko basin; D.b.—Delaware basin; M.b.—Midland basin. Gray outlines show locations of maps in Figures 5 and 8. Locations of sample sites discussed in the text are shown; some symbols represent multiple closely spaced samples.

This article reports new detrital-zircon data and summarizes previously published data from the Marathon foreland in order to identify the composition of the provenance of the clastic sediment. Previous interpretations (Gleason et al., 2007; Soreghan and Soreghan, 2013) have recognized a supply of detritus to Marathon clastic sediment from accreted Gondwanan sources. The Gondwanan Coahuila terrane is adjacent to the Marathon orogen and foreland (Fig. 1) and, therefore, appears to be the most likely provenance of Gondwanan origin. Initial synorogenic detritus prograded into the Marathon foreland in Mississippian time (e.g., Ross, 1986), heralding the approach of the subduction complex along the leading edge of the Coahuila terrane; closure of the ocean basin and docking of Coahuila on the Laurentian crustal margin followed in Early Permian time (e.g., Dickinson and Lawton, 2001). To evaluate the Coahuila terrane as the specific possible source of the Marathon foreland detritus, this article compares detrital-zircon data from the late Paleozoic synorogenic clastic sediment in the Marathon foreland with detrital-zircon data from proximal sandstones within the Coahuila terrane. The proximity of the Coahuila terrane to the Marathon orogenic foreland provides a unique opportunity to directly compare detrital-zircon populations from source (Coahuila) to sink (Marathon). Published U-Pb ages of zircons from igneous rocks in the Coahuila terrane (Lopez, 1997; Lopez et al., 2001; Poole et al., 2005) document potential primary sediment sources. A comparison of the detrital-zircon populations in the Marathon foreland with published data from the Delaware (Soreghan and Soreghan, 2013; Xie et al., 2018) and Anadarko (Thomas et al., 2016) intracratonic basins to the north provides a test of the extent of sediment dispersal onto the more distal craton of southern Laurentia (Fig. 1).

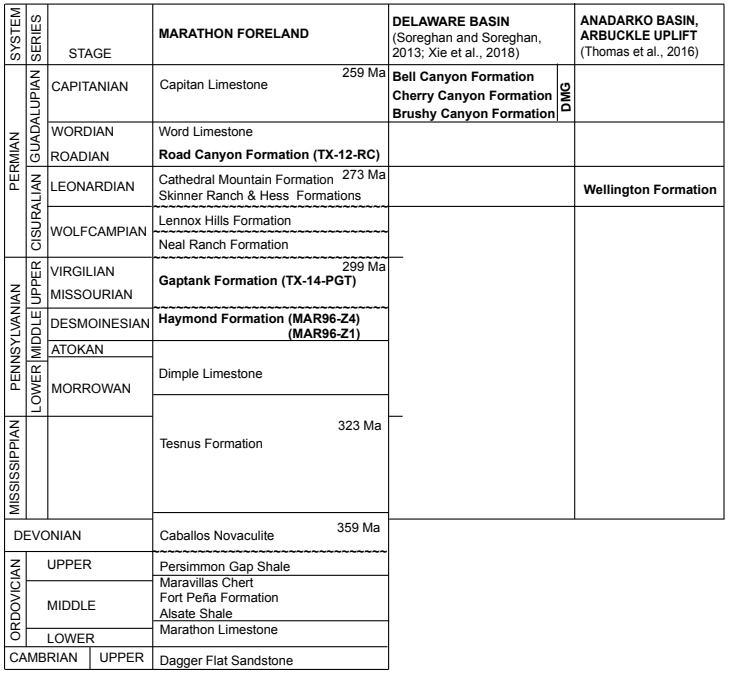

Figure 2. Stratigraphic columns for Marathon foreland, Delaware basin, and Anadarko basin. Names of sampled stratigraphic units are shown in bold type. DMG—Delaware Mountain Group. Time scale is ICS 2016 (Cohen et al., 2013, updated).

MARATHON FORELAND STRATIGRAPHY

The Marathon allochthon includes an Upper Cambrian to Lower Mississippian, off-shelf, deep-water, passive-margin succession of shale, sandstone, limestone, and chert (novaculite), as well as conglomerate and distinctive boulder beds (Fig. 2); carbonate clasts in the boulder beds reflect dispersal from an adjacent passive-margin shelf (King, 1937; McBride, 1989). Within the Marathon allochthon, a very thick synorogenic succession of muddy and sandy turbidites of Early Mississippian to Middle Pennsylvanian age overlies the Cambrian–Devonian, off-shelf, passive-margin succession (Fig. 2) (King, 1937; Ethington et al., 1989; McBride, 1989). Around the Marathon thrust front and in the proximal foreland, an unconformity-punctuated succession of Upper Pennsylvanian and Lower Permian shale, sandstone, and limestone records filling of the foreland basin (Ross, 1986).

The initial synorogenic deposits at the base of the Mississippian Tesnus Formation (Fig. 2) indicate an abrupt increase in supply of clastic sediment at the inception of orogeny (McBride, 1989). Tuff beds in the Tesnus Formation are consistent with evolution of a subduction complex and magmatic arc on the south (Imoto and McBride, 1990); however, no samples have been analyzed for crystallization ages. Above the Tesnus Formation, the Lower and Middle Pennsylvanian Dimple Limestone (Fig. 2) includes shallow-marine limestones along the leading part of the Marathon allochthon and carbonate turbidites deposited down a southerly slope (Ross, 1986).

Overlying the Dimple Limestone, the Middle Pennsylvanian (Desmoinesian) Haymond Formation (Fig. 2) is a thick succession of shaly and sandy turbidites (King, 1937; Denison et al., 1969; Ross, 1986; McBride, 1989). Deep-marine turbidites of the lower part of the Haymond Formation give way upward to shallow-marine and deltaic deposits in the upper part of the formation (Ross, 1986; McBride, 1989; Gleason et al., 2007), indicating transition from an underfilled basin to a filled basin near the top of the succession. Paleocurrent indicators generally show a complex array of directions that apparently include downslope fans, as well as slope-parallel contour currents (McBride, 1989; Gleason et al., 2007). During deposition of the Tesnus through Haymond succession, little or no synorogenic sediment spread onto the adjacent shelf; regional unconformities punctuate a very thin, Mississippian–Middle Pennsylvanian, starved-basin succession, which is capped by a Middle Pennsylvanian limestone (e.g., Hamlin, 2009).

The Haymond Formation contains boulder beds with boulders of three distinct types: intrabasinal fragments of older strata of the Marathon allochthon, metamorphic and igneous rocks from external sources, and limestone

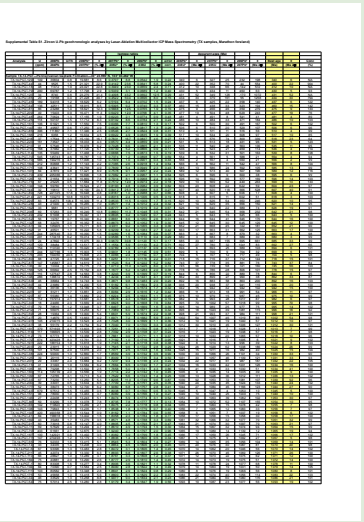

[1]Supplemental Table S1. U-Pb geochronologic analyses, Marathon foreland. Please visit https://doi.org/10.1130/GES02033.S1 or access the full-text article on www.gsapubs.org to view Table S1.

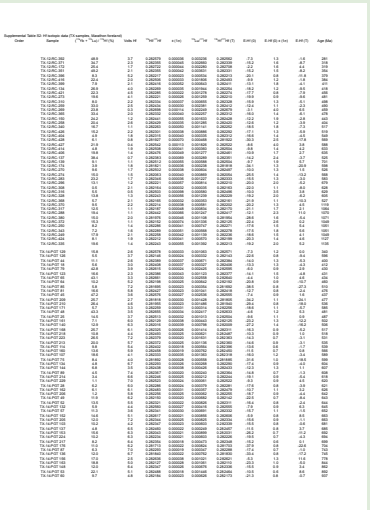

[2]Supplemental Table S2. Hf isotopic data, Marathon foreland. Please visit https://doi.org/10.1130/GES02033.S2 or access the full-text article on www.gsapubs.org to view Table S2.

boulders with middle Cambrian trilobites distinctive of the seaward edge of the passive-margin carbonate shelf (King, 1937; Denison et al., 1969; Palmer et al., 1984; Ross, 1986; McBride, 1989). The boulders include rhyolite (U-Pb zircon crystallization age of 371 ± 12 Ma with early to middle Proterozoic xenocrysts) and granodioritic gneiss (U-Pb zircon age of 1436 ± 160 Ma with 330 ± 72 Ma metamorphic overprint), suggesting derivation from a Devonian–Mississippian orogen with a Mesoproterozoic basement (Denison et al., 2005).

The Upper Pennsylvanian Gaptank Formation (Fig. 2), consisting of shallow-marine clastic and carbonate rocks, unconformably overlies the Haymond Formation along the leading edge of the Marathon allochthon (King, 1937; Ross, 1986; McBride, 1989), indicating significant pre-Gaptank thrust deformation of the synorogenic turbidites in the allochthon. The overlying Lower Permian (lower Wolfcampian) Neal Ranch Formation (Fig. 2) is discontinuously distributed between bounding unconformities. Along part of the thrust front, the Gaptank and Neal Ranch shallow-marine deposits grade laterally into a basinal facies ("Dugout beds"), indicating continued deposition of synorogenic turbidites around the leading edge of the allochthon (Ross, 1986).

The lower part of the Permian succession above the Gaptank Formation includes multiple unconformities that bracket sporadically distributed sedimentary packages (King, 1980; Ross, 1986). The leading Marathon thrust faults affect the Lower Permian (lower Wolfcampian) Neal Ranch Formation, and the upper Wolfcampian Lenox Hills Formation unconformably overlies thrust-deformed strata as young as early Wolfcampian (Neal Ranch Formation and the "Dugout beds"), bracketing the time of the latest significant movement on the Marathon frontal thrust faults (Ross, 1986). The Lenox Hills and younger Permian units, including the Road Canyon Formation (Fig. 2), constitute a postorogenic cover over the leading edge of the Marathon allochthon.

SAMPLE DISTRIBUTION AND DATA PRESENTATION FOR MARATHON FORELAND

Two new analyses for U-Pb ages (Supplemental Table S1[1]) and two previously published analyses (Gleason et al., 2007) document the detrital-zircon populations in the Marathon foreland (Figs. 3 and 4); the two new samples were also analyzed for Hf isotopic ratios (Figs. 3 and 4; Supplemental Table S2[2]). The previously published data are from samples of the deep-marine turbidite-fan facies and of the fan-delta facies in the Pennsylvanian Haymond Formation (Gleason et al., 2007). The new samples are from shallow-marine late-stage basin fill in the Upper Pennsylvanian Gaptank Formation and from the Middle Permian Road Canyon Formation, which unconformably overlies the youngest thrust-deformed beds in the Marathon foreland (Fig. 2). The samples are from the frontal thrust-belt structures and the most proximal foreland (Fig. 1). The data are described here in order of depositional age (oldest to youngest). For comparison of two possible sources of sediment, two separate plots show the data in the context of Laurentian (including Appalachian) age provinces (Fig. 3) and Gondwanan age provinces (Fig. 4).

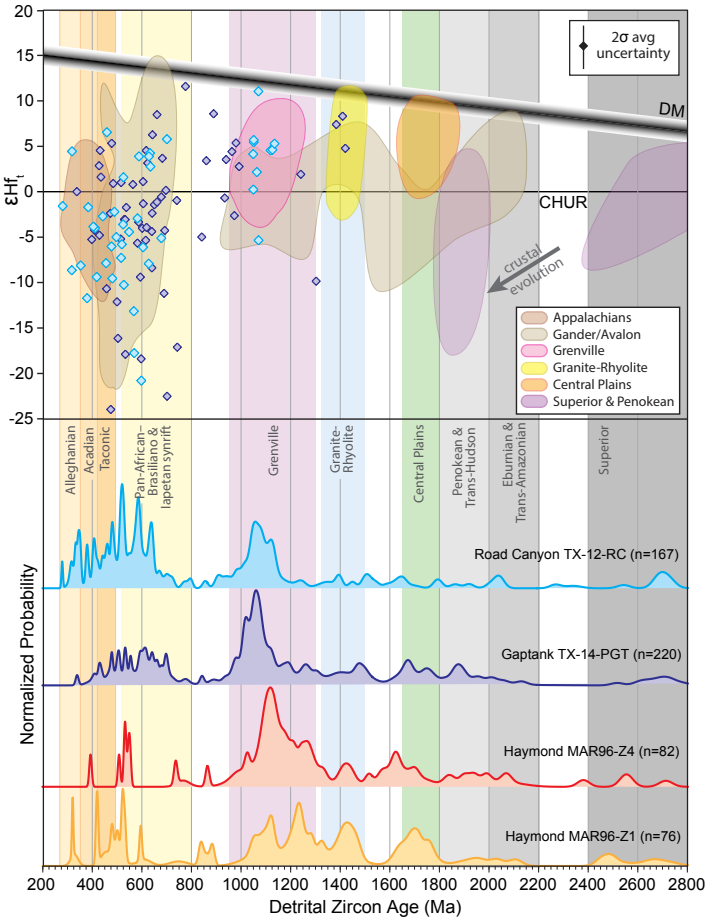

Figure 3. Relative U-Pb age-probability plots (lower panel) and Hf-evolution diagram (upper panel) showing results from analyses of Pennsylvanian–Permian sandstones in the Marathon foreland with respect to potential provenance provinces in the Appalachians and North American craton (age ranges shown by vertical color bands). Lower panel: Relative age-probability plots for four analyzed samples. For two new analyses, analytical data and location information are in Supplemental Tables S1 and S2 (see text footnotes 1 and 2); two previously published analyses are from Gleason et al. (2007). Upper panel: εHf$_t$ data for two samples (data points are color coded as shown in the lower panel); the average uncertainty of Hf isotopic analyses (2.6 epsilon units at 2σ) is shown in upper right. The Hf-evolution diagram shows the Hf isotopic composition at the time of zircon crystallization, in epsilon units, relative to the chondritic uniform reservoir (CHUR) (Bouvier et al., 2008) and to the depleted mantle (DM) (Vervoort et al., 1999). Shown for reference is the evolution of typical continental crust, which is based on a $^{176}Lu/^{177}Hf$ ratio of 0.0115 (Vervoort and Patchett, 1996; Vervoort et al., 1999). Reference fields summarize published Hf isotopic data for the Appalachians (Mueller et al., 2007, 2008) and accreted Gander and Avalon terranes (Willner et al., 2013, 2014; Pollock et al., 2015; Henderson et al., 2015), the Grenville orogen (Bickford et al., 2010; Gehrels and Pecha, 2014), Mesoproterozoic rocks of the Midcontinent Granite-Rhyolite province and Paleoproterozoic rocks of the Central Plains orogen (Goodge and Vervoort, 2006; Bickford et al., 2008; Gehrels and Pecha, 2014), and Penokean and Superior provinces of the Canadian Shield (Gehrels and Pecha, 2014).

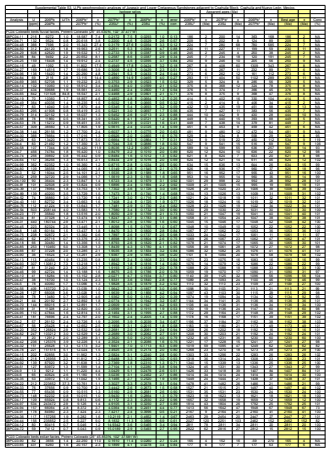

[3]Supplemental Table S3. U-Pb geochronologic analyses, adjacent to Coahuila block. Please visit https://doi.org/10.1130/GES02033.S3 or access the full-text article on www.gsapubs.org to view Table S3.

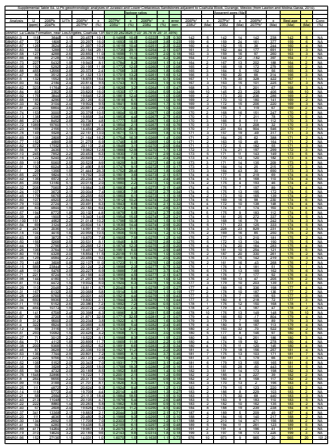

[4]Supplemental Table S4. U-Pb geochronologic analyses, adjacent to Coahuila block (from Lawton and Molina-Garza, 2014). Please visit https://doi.org/10.1130/GES02033.S4 or access the full-text article on www.gsapubs.org to view Table S4.

Detrital-zircon U-Pb age data from proximal sandstones, as well as U-Pb age data from igneous rocks, characterize the zircon populations available within the Coahuila terrane as a possible provenance of Marathon detritus. New U-Pb analyses of 10 samples (Supplemental Table S3[3]), along with published data from four other samples (Supplemental Table S4[4], data from Lawton and Molina-Garza, 2014; Supplemental Table S5[5], data from Gray et al., 2008), from Upper Jurassic–Lower Cretaceous proximal sandstones derived from uplifted blocks within the Coahuila terrane characterize locally derived detritus within the terrane. In addition, previously published analyses of U-Pb ages of volcanic and plutonic rocks in and around the Coahuila terrane (Fig. 1) characterize potential primary sources of Marathon detritus.

SANDSTONE PETROGRAPHY OF MARATHON SAMPLES

Gaptank Formation (Sample TX-14-PGT)

Sample TX-14-PGT (30°23.996′ N, 103°03.262′ W) is from a meter-thick sandstone bed in the uppermost Gaptank Formation in the frontal part of the Marathon thrust belt (Fig. 5). Within a succession of five limestone units separated by sandstone and shale (King, 1980), the sandstones contain abundant fossil fragments (McBride, 1964). The Gaptank Formation overall represents a synorogenic, shoaling-upward succession of fluvial to marine shelf and shelf-edge deposits (King, 1930; McBride, 1964; Ross, 1967; Muehlberger and Tauvers, 1989).

Sample TX-14-PGT is an orange-brown weathering, medium-tan, hard, well-cemented lithic arenite of diverse composition with 0.1–0.2 mm subrounded, equant grains. Four hundred framework grains and 578 total grains and cement crystals were point-counted (Fig. 6). Framework grains are 36% monocrystalline quartz, 9.5% polycrystalline quartz, and 6.5% chert. Limestone grains and volcanic rock fragments are abundant, comprising 23% and 14%, respectively, of all framework grains. Feldspar grains are a significant component of this sample: 5% plagioclase, 4% untwinned feldspar, and 2% potassium feldspar. Calcite cement constitutes 31% of all points counted. Some calcite cement patches may be small, recrystallized limestone grains; limestone grains are typically recrystallized. Sparse shell fragments are preserved as sparry calcite-filled voids. Conglomerate beds in the lowermost part of the Gaptank Formation contain chert clasts derived from the Ordovician Maravillas Formation and Devonian Caballos Novaculite in the Marathon thrust belt to the south, which may also be the source of chert framework grains in sample TX-14-PGT.

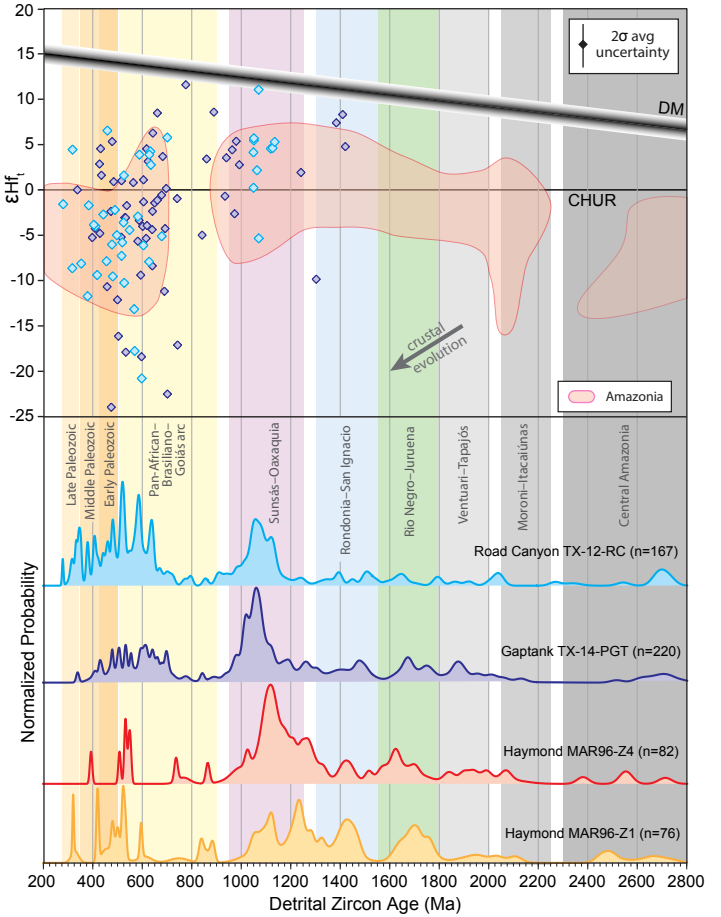

Figure 4. Presentation of the same relative U-Pb age-probability plots (lower panel) and Hf-evolution diagram (upper panel) as in Figure 3, but with respect to potential provenance provinces in the Coahuila terrane and Amazonia/Gondwana (age ranges shown by vertical color bands). Design of the figure is the same as described in the caption for Figure 3. Age brackets older than 500 Ma are compiled from Cordani et al. (2000), Tassinari et al. (2000), Cordani and Teixeira (2007), Cardona et al. (2010), Cristofolini et al. (2012), and Pepper et al. (2016). Age brackets younger than 500 Ma are matched to age data from the Coahuila and nearby Gondwanan accreted terranes; the early, middle, and late Paleozoic brackets correspond in age to the Taconic, Acadian, and Alleghanian events in the Appalachian orogen, but lateral continuity or genetic relationships are not established or implied. Reference fields summarize published Hf isotopic data for Amazonia (Pepper et al., 2016).

Road Canyon Formation (Sample TX-12-RC)

Sample TX-12-RC (30°21.503′ N, 103°14.137′ W) is from the Road Canyon Formation in the Marathon foreland (Fig. 5), stratigraphically above unconformities that truncate the youngest folded beds in the Marathon thrust belt. The sample is from the lower part of a sandstone interval, which includes two limestone beds. Overall, the Road Canyon Formation consists of lenticular limestone conglomerate overlain by fissile siltstone interbedded with fine-grained

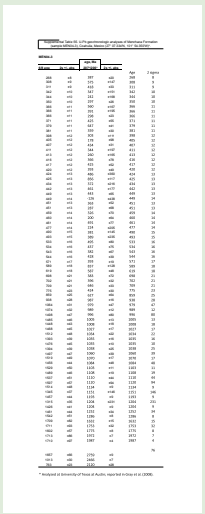

[5]Supplemental Table S5. U-Pb geochronologic analyses, Menchaca Formation, Coahuila (from Gray et al., 2008). Please visit https://doi.org/10.1130/GES02033.S5 or access the full-text article on www.gsapubs.org to view Table S5.

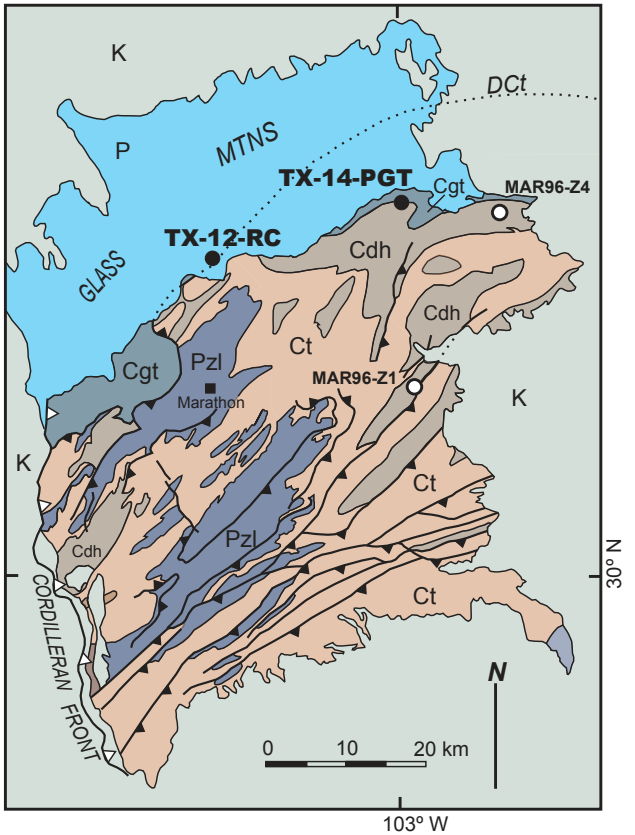

Figure 5. Geologic map of Marathon foreland showing locations of zircon-yielding sandstone samples described in the text. Map units: Pzl—lower Paleozoic rocks, Ct—Mississippian–Pennsylvanian Tesnus Formation, Cdh—Pennsylvanian Dimple and Haymond Formations, Cgt—Pennsylvanian Gaptank Formation, P—Permian strata, K—Cretaceous strata. Structures: DCt—Dugout Creek overthrust, the northwestern-most exposed Marathon-Ouachita thrust fault, dotted where covered; black teeth on faults—late Paleozoic Marathon-Ouachita thrust faults; white teeth on fault—Late Cretaceous–Tertiary Cordilleran reverse fault. Map compiled from King (1980) and Muehlberger and Tauvers (1989).

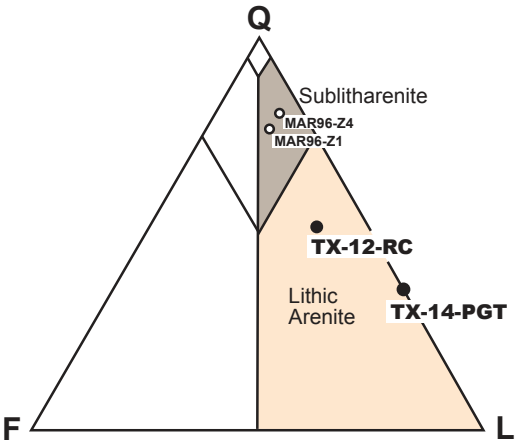

Figure 6. QmFLt plot of point-counted sandstone samples: Qm—monocrystalline quartz, F—feldspar, Lt—total rock fragments, including chert and polycrystalline quartz. Arenite names and boundaries are from Pettijohn et al. (1987).

sandstone and graded and laminated crinoid rudstone and packstone beds, representing debris-flow and turbidite deposition (Ross, 1986; Jansen, 2014).

Sample TX-12-RC is a reddish-brown weathering, brownish-tan, well-cemented lithic arenite with 0.1-mm-diameter rounded and subrounded grains. In total, 215 framework grains were point-counted plus five additional cement patches (Fig. 6). Carbonate rock fragments recrystallized to dolomite comprise 62.8% of framework grains. Almost all other framework grains are quartz: 13.5% monocrystalline quartz and 21.9% chert. Large patches of coarsely crystalline dolomite, commonly in rhombs, are interpreted to be recrystallized carbonate rock fragments because rounded grains of identical composition are common.

Haymond Formation

The Haymond Formation includes a lower foredelta submarine-ramp turbidite facies and an upper delta-front and delta-plain fan-delta facies in tight folds within the Marathon thrust belt (Fig. 5) (Gleason et al., 2007). Gleason et al. (2007) described and point-counted one sample from each facies (Fig. 6). Both samples were sublitharenites of similar compositions. In descriptions summarized from Gleason et al. (2007), sample MAR96-Z1 from the lower facies contains 70% monocrystalline quartz and 7% polycrystalline quartz grains. Feldspar comprises 9% of framework grains. Sedimentary rock fragments, mainly slate-phyllite fragments and mudrock grains, make up 13% of framework grains. Detrital matrix makes up 7% of MAR96-Z1. Sample MAR96-Z4 contains 74% monocrystalline quartz grains and 7% polycrystalline quartz. Feldspar makes up 5% of this sample. Slate-phyllite and mudrock sedimentary rock fragments comprise 12% of grains. Detrital matrix makes up only 2% of MAR96-Z4. MAR96-Z1 consists of fine-grained subangular to subrounded grains. MAR96-Z4 and other upper Haymond sandstones consist of fine- to medium-grained subangular to subrounded grains. Unlike the Gaptank and Road Canyon samples, neither Haymond sample has calcite cement or carbonate rock fragments.

ANALYTICAL METHODS

Sample Collection and Processing

An ~12 kg mass of medium- to coarse-grained sandstone was collected from a restricted stratigraphic interval for each detrital-zircon sample and then processed utilizing methods outlined by Gehrels (2000), Gehrels et al. (2008), Gehrels and Pecha (2014), and Thomas et al. (2017). Zircon grains were extracted using traditional methods of jaw crushing and pulverizing, followed by density separation using a Wilfley table. The resulting heavy-mineral fraction was further purified using a Frantz LB-1 magnetic barrier separator and heavy liquids. A representative split of the zircon yield was incorporated into a 2.54 mm epoxy mount along with multiple fragments of the U-Pb primary standards Sri Lanka SL-F, FC-1, and R33, and Hf standards R33, Mud Tank, FC-1, Plesovice, Temora, and 91500. The mounts were sanded down ~20 μm, polished to 1 μm, and imaged by backscattered electrons (BSE) and cathodoluminescence (CL) using a Hitachi 3400N scanning electron microscope (SEM) and a Gatan Chroma CL2 detector system at the Arizona LaserChron SEM Facility (https://www.microscopy.arizona.edu). Prior to isotopic analysis, mounts were cleaned in an ultrasonic bath of 1% HNO_3 and 1% HCl in order to remove surficial common Pb.

U-Pb Geochronologic Analysis

U-Pb geochronology of individual zircon crystals was conducted by laser ablation–inductively coupled plasma–mass spectrometry (LA-ICP-MS) at the Arizona LaserChron Center (www.laserchron.org). The isotopic analyses involved ablation of zircon using a Photon Machines Analyte G2 excimer laser coupled to either a Thermo Element2 single-collector ICP-MS or a Nu Instruments multicollector ICP-MS. Ultrapure helium carried the ablated material from the HelEx cell into the plasma source of each ICP-MS.

Analyses conducted with the Nu ICP-MS utilized Faraday collectors for measurement of ^{238}U and ^{232}Th, either Faraday collectors or ion counters for ^{208}Pb, ^{207}Pb, and ^{206}Pb, and ion counters for ^{204}(Pb, Hg) and ^{202}Hg (see Supplemental Table S1 [footnote 1] for specific methods used for each sample), depending on grain size. For larger grains, a 30-μm-diameter spot was used, and masses 206, 207, 208, 232, and 238 were measured with Faraday detectors, whereas the smaller 202 and 204 ion beams were measured with ion counters. The acquisition routine included a 15 s integration on peaks with the laser off (for backgrounds), fifteen 1 s integrations with the laser firing, and a 30 s delay to ensure that the previous sample was completely purged from the system. Smaller grains were analyzed with all Pb isotopes in ion counters, using a 20 μm beam diameter, and consisted of a 12 s integration on peaks with the laser off (for backgrounds), twelve 1 s integrations with the laser firing, and a 30 s delay to purge the previous sample.

Analyses conducted with the Element2 ICP-MS utilized a single scanning electron multiplier that sequences rapidly through U, Th, and Pb isotopes. Ion intensities are measured in pulse-counting mode for signals less than 50,000 cps (counts per second), in both pulse-counting and analog mode for signals between 50,000 and 5×10^6 cps, and in analog mode above 5×10^6 cps. The calibration between pulse-counting and analog signals is determined line-by-line for signals between 50,000 and 5×10^6 cps, and it is applied to $>5 \times 10^6$ cps signals. Four intensities were determined and averaged for each isotope, with dwell times of 0.0052 s for 202, 0.0075 s for 204, 0.0202 s for 206, 0.0284 s for 207, 0.0026 s for 208, 0.0026 s for 232, and 0.0104 s for 238. With the laser set at an energy density of ~5 J/cm^2, a repetition rate of 8 Hz, and an ablation time of 10 s, ablation pits were ~12 μm in depth. Sensitivity with these settings is ~5000 cps/ppm. Each analysis consisted of 5 s on peaks with the laser off (for backgrounds), 10 s with the laser firing (for peak intensities), and a 20 s delay to purge the previous sample and save files.

Analyses with one U-Th-Pb measurement per grain were conducted on 167–220 grains from the samples from the Marathon foreland and on 94–117 grains from the samples from Coahuila. Grains were selected in random fashion; crystals were rejected only if they contained cracks or inclusions or were too small to be analyzed. The use of high-resolution BSE and CL images provided assistance in grain selection and spot placement.

Data reduction was accomplished using Agecalc (a Microsoft Excel spreadsheet), which is the standard Arizona LaserChron Center reduction protocol (Gehrels et al., 2008; Gehrels and Pecha, 2014). Data were filtered for discordance, $^{206}Pb/^{238}U$ precision, and $^{206}Pb/^{207}Pb$ precision as indicated in the notes in Supplemental Tables S1, S3, and S4 (see footnotes 1, 3, and 4). For this data set, the average precision of individual ages is 3.5% (2σ). Including external (systematic) uncertainties yields an average accuracy of 3.9% (2σ). Data are presented on normalized age-probability diagrams, which sum all relevant analyses and uncertainties and divide each curve by the number of analyses, such that all curves contain the same area. Age groups are characterized by the ages of peaks in age probability and by the range of constituent ages.

Hf Isotopic Analysis

Hf isotopic analyses were conducted utilizing the Nu multicollector LA-ICP-MS system at the Arizona LaserChron Center following methods reported by Cecil et al. (2011) and Gehrels and Pecha (2014). On average, 56 Hf analyses were conducted for each sample from the Marathon foreland. Grains were selected to represent each of the main age groups and to avoid crystals with discordant or imprecise ages. CL images were utilized to ensure that all Hf analyses were within the same growth domain as the U-Pb pit, although in most analyses, Hf laser pits were located directly on top of the U-Pb analysis pits. Complete Hf isotopic data and Hf evolution plots of individual samples are presented in Supplemental Table S2 (see footnote 2).

Hf data are presented using Hf evolution diagrams (Figs. 3 and 4), where initial $^{176}Hf/^{177}Hf$ ratios are expressed in εHf_t notation, which represents the Hf isotopic composition at the time of zircon crystallization relative to the

chondritic uniform reservoir (CHUR) (Bouvier et al., 2008). Internal precision for $^{176}Hf/^{177}Hf$ and εHf_t is reported for each analysis on Hf evolution plots in Supplemental Table S2 and as the average for all analyses (2.2 epsilon units at 2σ) on Figures 3 and 4. On the basis of the in-run analysis of zircon standards, the external precision is 2–2.5 epsilon units (2σ). Hf isotopic evolution of typical continental crust is shown with arrows on εHf_t evolution diagrams, based on a $^{176}Lu/^{177}Hf$ ratio of 0.0115 (Vervoort and Patchett, 1996; Vervoort et al., 1999).

Our Hf isotope data are interpreted within the standard framework of juvenile (positive) values indicating magma consisting mainly of material extracted from the mantle during or immediately prior to magmatism, versus more evolved (negative) values that record incorporation of significantly older crust. Vertical arrays on εHf_t diagrams are interpreted to represent magmas that contain both material derived from the mantle during (or immediately prior to) magmatism and significantly older crustal materials.

RESULTS OF DETRITAL-ZIRCON ANALYSES FROM MARATHON SAMPLES: U-Pb AGE DATA AND Hf ISOTOPIC DATA

Haymond Formation (Sample MAR96-Z1; Gleason et al., 2007)

A sandstone from the turbidite-fan facies of the Haymond Formation (sample MAR96-Z1; Gleason et al., 2007) has a dominant concentration of detrital-zircon ages between 1470 Ma and 1026 Ma with peaks at 1123, 1235, and 1438 Ma (Figs. 2–5). Secondary concentrations are at 1778–1632 Ma with a peak at 1708 Ma and at 533–452 Ma with a peak at 523 Ma. Older grains include minor concentrations at 2105–1908 Ma and at 2718–2453 Ma and a single grain at 3026 Ma. Younger ages include two grains each at 423–419 Ma and at 329–323 Ma.

Haymond Formation (Sample MAR96-Z4; Gleason et al., 2007)

A sandstone from the fan-delta facies of the Haymond Formation (sample MAR96-Z4; Gleason et al., 2007) has a dominant concentration of detrital-zircon ages between 1438 Ma and 1020 Ma (mostly between 1331 Ma and 1020 Ma) with peaks at 1123, 1247, and 1438 Ma (Figs. 2–5). Secondary concentrations are at 2106–1839 Ma with no distinct peak and at 1738–1567 Ma with a peak at 1624 Ma. A few older grains are scattered between 2709 Ma and 2379 Ma. A younger secondary concentration is at 553–509 Ma with a peak at 532 Ma; a single grain has an age of 394 Ma. The detrital-zircon populations of the two Haymond samples are similar, suggesting a common provenance (Gleason et al., 2007).

Gaptank Formation (Sample TX-14-PGT)

A sample of sandstone from the Upper Pennsylvanian Gaptank Formation is from near the leading edge of the Marathon thrust belt (Figs. 2–5). The sample has a strongly dominant mode of detrital-zircon ages at 1147–936 Ma with a peak at 1020 Ma (Figs. 3 and 4). A secondary concentration at 745–340 Ma has multiple subequal peaks and a strong peak at 557 Ma. A wide spread of ages between 2131 Ma and 1156 Ma has peaks at 1870, 1752, 1678, 1475, and 1268 Ma. Another minor concentration at 3217–2598 Ma has peaks at 2726 Ma and 2685 Ma.

Hf isotopic data for Precambrian grains generally conform to crustal evolution trends with some exceptions toward more negative εHf_t values (Figs. 3 and 4). For zircon grains in the age range 745–500 Ma, εHf_t values range from +8.5 to –27.3 and cluster around +1.0 to –5.7, consistent with involvement of older crust in the source of the magmas. Zircon grains in the age range of 500–340 Ma have εHf_t values between +5.3 and –24.1, indicating variable sources.

Road Canyon Formation (Sample TX-12-RC)

The Middle Permian Road Canyon Formation is stratigraphically above the angular unconformity that marks the youngest age of Marathon thrusting. The sample, representing early postorogenic unroofing, is from near the leading edge of the buried Marathon thrust belt (Figs. 2–5). The sample has a strongly dominant mode of detrital-zircon ages at 706–280 Ma with important peaks at 588 Ma and 522 Ma, as well as other strong peaks at 640 Ma and 348 Ma (Figs. 3 and 4). Another important concentration at 1134–907 Ma has a strong peak at 1064 Ma. The dominance of the 588–522 Ma peaks over the 1064 Ma peak is unusual for detrital-zircon populations in most of North America. Ages are scattered from 2132 Ma to 1134 Ma with a peak at 2044 Ma. Another secondary concentration at 2728–2677 Ma has a peak at 2686 Ma. The sample has two older grains at 3490 Ma and 3087 Ma.

Hf isotopic data for Precambrian grains generally conform to crustal evolution trends with some exceptions toward more positive εHf_t values (Figs. 3 and 4). For zircon grains in the age range 745–500 Ma, εHf_t values range from +5.7 to –20.9 and cluster around –3 to –8, consistent with involvement of older crust in the source of the magmas. Zircon grains in the age range of 500–340 Ma have εHf_t values that range from +6.5 to –11.8 and cluster around –2.3 to –7.9, indicating assimilation of older continental crust.

PROVENANCE OF MARATHON DETRITUS

The U-Pb ages of detrital zircons from the Marathon foreland sandstones correspond in age to major provinces of Gondwana, as well as to the ages of major provinces of Laurentia (Figs. 3 and 4). The Marathon detrital-zircon populations include age equivalents of all three (Taconic, Acadian, and Alleghanian) Appalachian orogenic events (Fig. 3), and these ages are roughly matched by ages of Paleozoic orogenic events in Gondwana (Fig. 4). Prominent concentrations of ages between 740 Ma and 500 Ma correspond in age to Pan-African–Brasiliano–Goiás arc (termed simply Pan-African throughout the text and fully identified in the figures) components of Gondwanan accreted

terranes (Fig. 4); however, the same age range includes the ages of Iapetan synrift igneous rocks of the Laurentian margin (Fig. 3), specifically synrift igneous rocks along the Southern Oklahoma fault system (e.g., Gleason et al., 2007). A strong to dominant age peak in the Marathon samples matches the age of the Sunsás province of Gondwana (Fig. 4), which corresponds in age to the Grenville province of Laurentia (Fig. 3). The Marathon samples have a scattering of ages and minor peaks between 2050 Ma and 1300 Ma, spanning the ages of several provinces of the Amazonian and Laurentian cratons. Older zircons range in age from 3490 Ma to 2550 Ma, corresponding to the Central Amazonian province of Gondwana and to the Superior and Wyoming provinces of Laurentia. The overlap of ages of major provinces of Laurentia with those of Gondwana precludes definitive assignment of Marathon zircon grains to specific sources. As a result, some of these ages have been interpreted to represent accreted Gondwanan terranes, whereas others have been interpreted to be from sources in Laurentia, especially the Appalachians (e.g., Gleason et al., 2007; Soreghan and Soreghan, 2013).

Although a clear distinction between Laurentian (Appalachian) and Gondwanan (Amazonia) sources is not supported by U-Pb ages of zircons, εHf_t values have distinctive aspects that do suggest discrimination between the alternatives for the possible provenance (Fig. 7). For grains with ages of the Paleozoic orogens, those from the Appalachians mostly have positive εHf_t values, whereas those from Amazonia generally have more negative values. The Marathon samples have mostly negative values, suggesting crustal evolution more like that of Amazonia. Zircons from the Marathon foreland with ages of 750–500 Ma generally have negative εHf_t values, similar to those of Pan-African components of Gondwana, and in contrast to the strongly positive εHf_t values of zircons from synrift Wichita granites in the Southern Oklahoma fault system along the Iapetan rifted margin of Laurentia (Fig. 7) (Thomas et al., 2016). Appalachian and Gondwanan zircons overlap in the 2σ data density for ages younger than 750 Ma; however, the data are clearly separated at the 1σ level (Fig. 7B). Peak density for samples from the Marathon foreland corresponds closely to Amazonia data at the 1σ level (Fig. 7B). Nearly all zircons with Grenville ages (1300–950 Ma) from the Appalachians have positive εHf_t values, although a few grains have negative values; Appalachian 1σ data density plots completely in the positive for εHf_t (Fig. 7B). Grains with Sunsás ages (1250–950 Ma) from Amazonia have a wide range of εHf_t values, but a substantial proportion has values more negative than those of the Appalachians (Fig. 7). Similarly, zircons from the Marathon samples have a wide range of εHf_t values, but several are in the more negative range and are, thus, more like those of Amazonia (Gondwana). For ages older than 1300 Ma, the Appalachian 2σ data density shows mostly positive εHf_t, whereas Amazonia plots largely negative at the 1σ and 2σ levels (Fig. 7). The Marathon samples generally have more negative εHf_t values, similar to those of Gondwanan zircons (Fig. 7).

The general U-Pb and εHf_t characteristics discussed here suggest a Gondwanan source for detritus in the Marathon foreland, but more specific comparisons are needed. The most obvious proximal source of Gondwanan detritus is the Coahuila terrane in the internal part of the Marathon orogen (Fig. 1); a detailed characterization of Coahuila as a potential provenance for Marathon detritus follows.

Coahuila Terrane and Coahuila Block

The distribution and nature of pre-Cretaceous rocks in the crustal domain south of the Marathon suture zone and north of an inferred Jurassic left-lateral fault system in the southern part of the states of Coahuila and Nuevo León, Mexico, are incompletely known because of extensive cover of Lower Cretaceous carbonate strata and younger rocks (Figs. 1 and 8). Differing interpretations of the distributions and origins of older rocks have led to an array of names for the region, including Coahuila terrane (Campa and Coney, 1983; Ortega-Gutierrez et al., 1995), Coahuiltecano and Tarahumara terranes (Sedlock et al., 1993), and Coahuila block (Dickinson and Lawton, 2001). Recognizing that the crustal domain contains a number of tectonic elements that might generate different suites of detrital-zircon ages, we use the original general name of Coahuila terrane (Fig. 1). Gravity models show that the Coahuila terrane has a full thickness of continental crust (e.g., Keller et al., 1989a). A suture zone of deformed metasedimentary rocks, which apparently is a southwestward along-strike extension of the interior metamorphic belt of the Ouachita-Marathon orogen (Fig. 1), separates the accreted Coahuila continental terrane from the Marathon sedimentary thrust belt on Laurentian continental crust. The Coahuila terrane includes Pennsylvanian–Permian mass-gravity marine turbidites and conglomerates, as well as volcanic rocks (McKee et al., 1988; Poole et al., 2005). The Las Delicias continental-margin magmatic arc (Fig. 1) formed on the overriding plate during the southward subduction of the Laurentian plate beneath the Coahuila terrane (Lopez, 1997; Poole et al., 2005).

The term "Coahuila block," as used here, applies to a structural element within the Coahuila terrane; the Coahuila block is composed of Paleozoic and older sedimentary and basement rocks unconformably overlain by Cretaceous strata (Fig. 8) (e.g., Eguiluz de Antuñano, 2001), which did not completely overlap the block until the late Albian (Las Uvas Formation, Fig. 9) (Humphrey and Díaz, 2003). The block has an abrupt northern boundary at the San Marcos fault zone (Fig. 8), a complex fault system that had recurrent activity during Jurassic–earliest Cretaceous and Late Cretaceous–Paleogene times (Charleston, 1981; McKee et al., 1984, 1990; Chávez-Cabello et al., 2005). The San Marcos fault zone separates the Coahuila block from the Sabinas basin or Coahuila fold belt (Charleston, 1981). The Coahuila block plunges southeastward, is flanked on the southern margin by the Parras transverse sector of the Mexican orogen (Fig. 8) (e.g., Fitz-Díaz et al., 2018), and probably ends in the subsurface at the Monterrey salient of the orogen, which overlies Middle to Upper Jurassic salt (Eguiluz de Antuñano et al., 2000). The western edge of the Coahuila block is concealed beneath Paleogene volcaniclastic rocks and Neogene basin fill and is not well defined. Although the Coahuila block is spatially extensive (on the order of 45,000 km^2), it represents only a fraction of the area of the Coahuila terrane (Fig. 1).

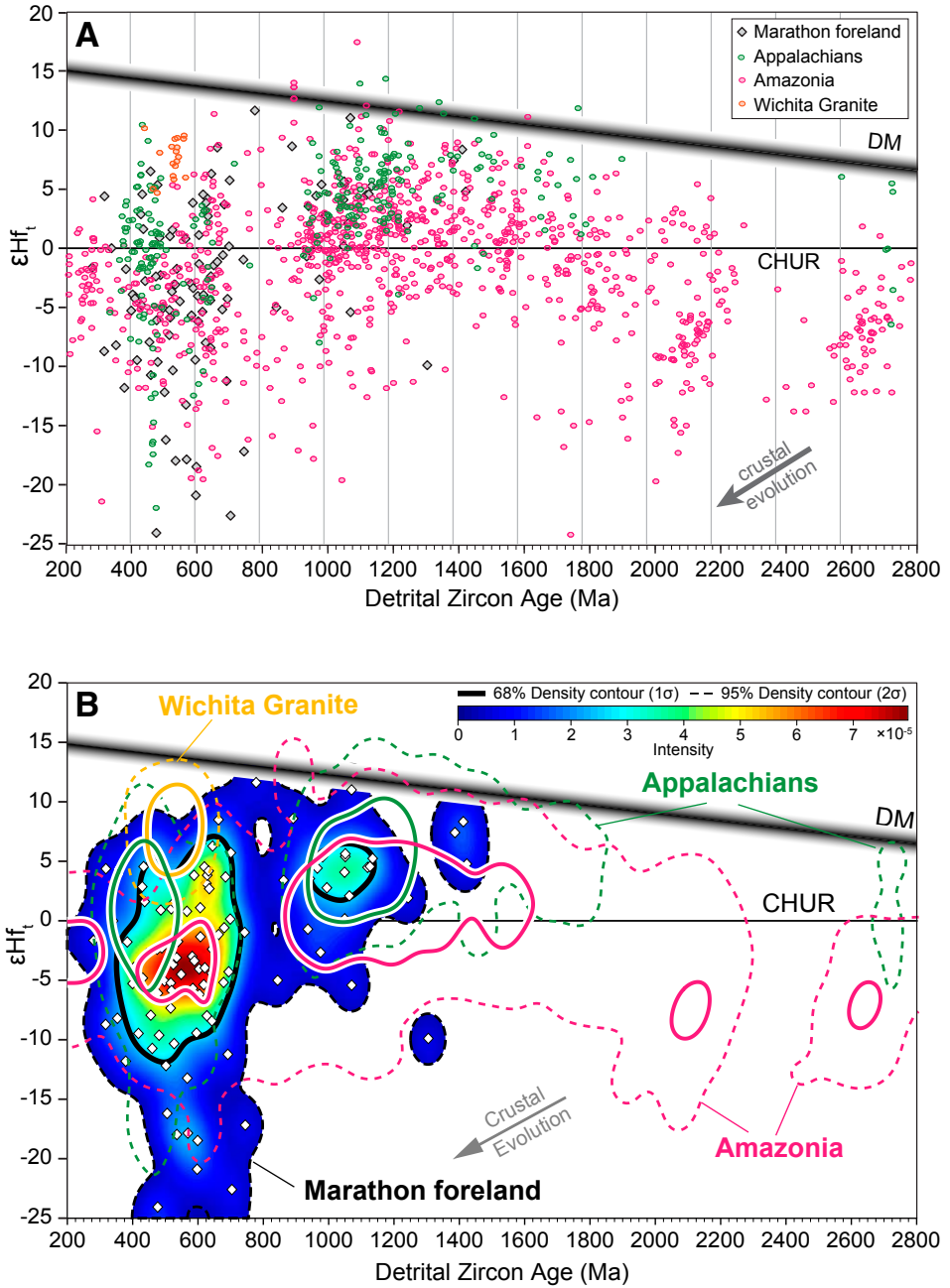

Figure 7. (A) Plot of εHf$_t$ data to compare results from Laurentia and the Appalachians (from sources listed in caption for Fig. 3), Gondwana/Amazonia (from Pepper et al., 2016), Southern Oklahoma igneous rocks (from Thomas et al., 2016), and Marathon foreland (from Fig. 3; Supplemental Table S2 [see text footnote 2]). The Appalachian data exclude identified Gondwanan accreted terranes in the Appalachian internides but include detrital zircons from Gondwanan sources in the Appalachian foreland (from Thomas et al., 2017). The Amazonia data are from various primary sources in South America (from Pepper et al., 2016). Data from the Wichita granites show the distinctive positive εHf$_t$ values for lapetan synrift rocks (Thomas et al., 2016). (B) Age-εHf$_t$ plotted as normalized bivariate kernel density estimates (KDEs) using HafniumPlotter version 1.4 (https://github.com/kurtsundell/HafniumPlotter). Construction of bivariate KDEs follows the same basic formulation as standard KDEs (Silverman, 1986). Each age-εHf$_t$ data point is converted into a three-dimensional Gaussian with kernel bandwidths of 50 m.y. along the *x* axis (U-Pb age) and 2 epsilon units along the *y* axis (εHf$_t$ value). All bivariate KDEs are mapped to a two-dimensional *x*-*y* grid of 512 × 512 cells, each with a single intensity value along the *z* axis. When viewed parallel to the *z* axis, bivariate KDEs produce an intensity map that can be contoured to specified intervals, which facilitates comparison of data clusters through nonarbitrary contouring of those clusters. Contours are plotted at 68% and 95% (1σ and 2σ) of peak density. Note the similarity between the Amazonia 1σ contour (bold magenta line) and peak density of the Marathon foreland (dark-red intensity values). DM—depleted mantle; CHUR—chondritic uniform reservoir.

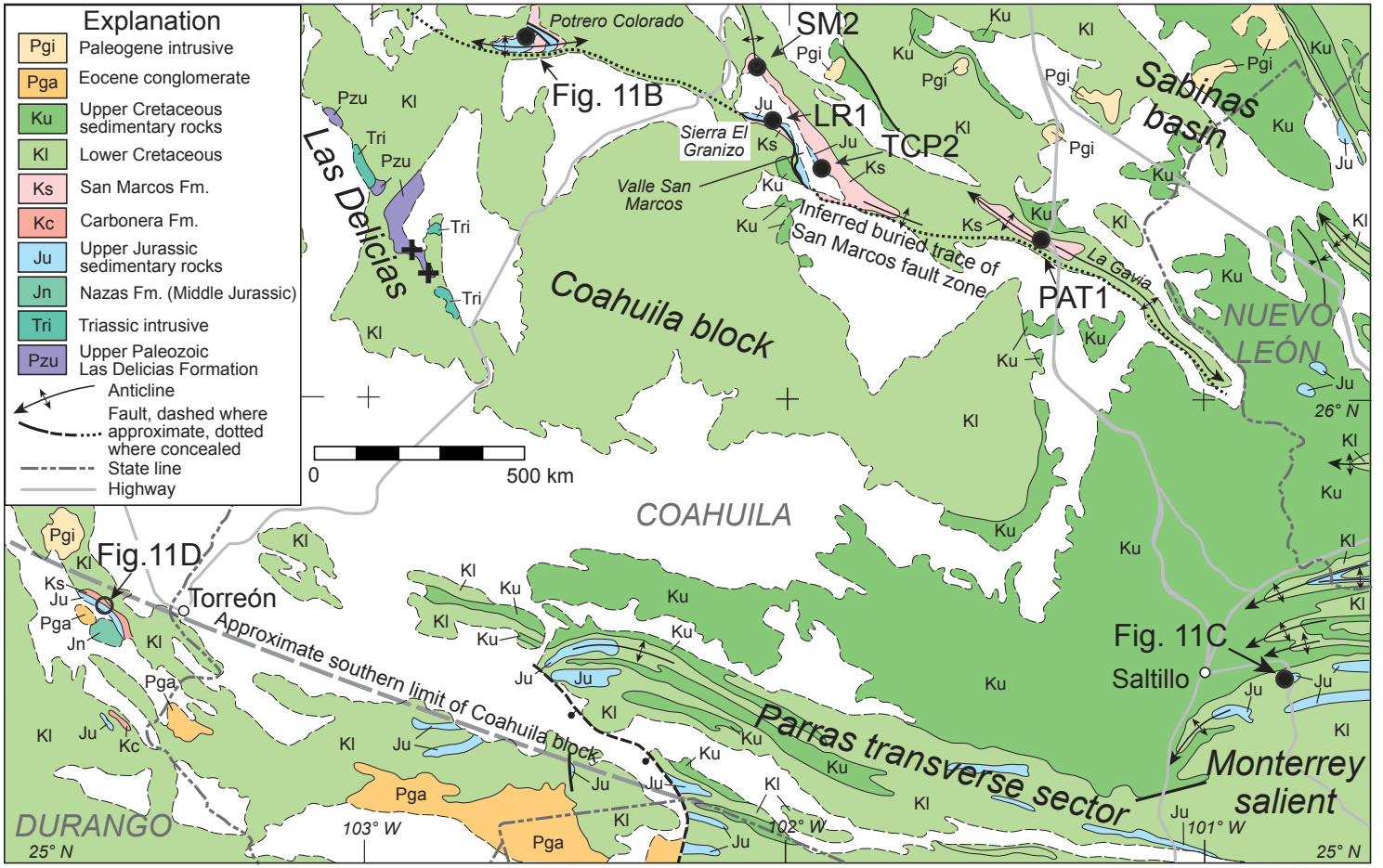

Figure 8. Location map of Coahuila block and vicinity, Coahuila and Nuevo León, Mexico. Geologic map adapted from regional geologic maps (Dirección General de Geografía del Territorio Nacional, 1980a, 1980b, 1982) and McKee et al. (1988). Trace of San Marcos fault zone, which marks the northern boundary of the Coahuila block and is only locally exposed, adapted from McKee et al. (1984), Chávez-Cabello et al. (2005), and González-Naranjo et al. (2008). Southern edge of Coahuila block inferred from magnetic map of Mexico (Servicio Geológico Mexicano, 2005). Symbols for sample sites are same as in Figure 1. Some site symbols indicate single samples (labeled with sample numbers); some site symbols represent multiple closely spaced samples (labeled with parts of Fig. 11).

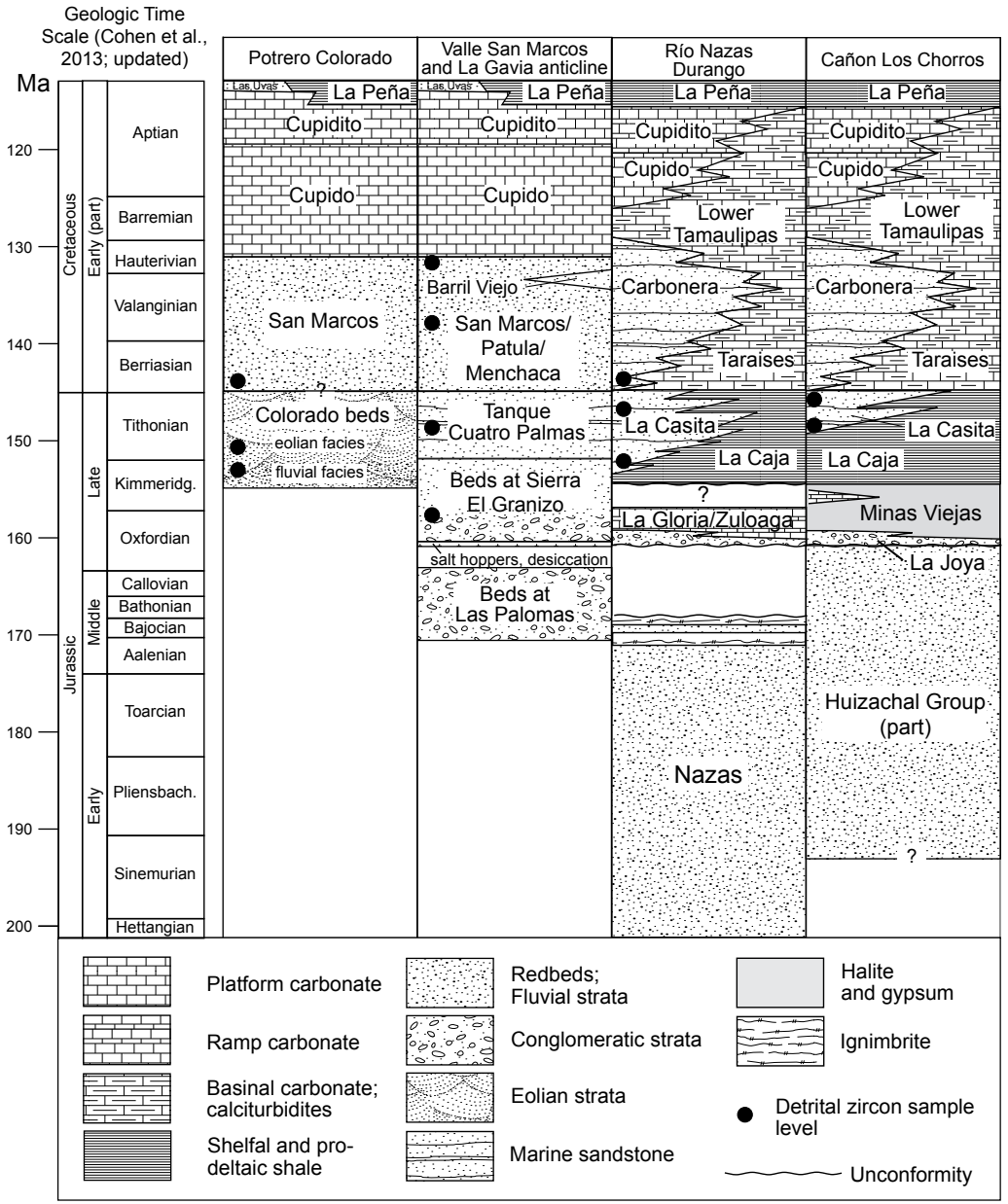

Figure 9. Correlation of Jurassic and Lower Cretaceous stratigraphic units sampled adjacent to the Coahuila block. Ages of stratigraphic units and implied lateral equivalents are from McKee et al. (1999), Eguiluz de Antuñano (1989, 2001), and Lawton and Molina-Garza (2014). Time scale is ICS 2016 (Cohen et al., 2013, updated).

Proximal siliciclastic deposits along the northern, southern, and southeastern sides of the Coahuila block indicate that it was a paleogeographic peninsula or island during Jurassic through mid-Aptian time (Smith, 1981; McKee et al., 1984, 1990; Eguiluz de Antuñano, 2001). A separate island was located in what is now the Sabinas basin at Potrero La Mula (Fig. 1) (Jones et al., 1984). Sediments derived directly from exposed rocks of the Coahuila block (McKee et al., 1990) are characterized by abrupt facies changes, particularly along the San Marcos fault zone at the northern flank of the block (Fig. 8), consistent with deposition in a rift or pull-apart setting. Depositional systems range through alluvial fans, ephemeral rivers, a small erg, and marginal marine settings that include fan deltas (e.g., Fortunato and Ward, 1982; McKee et al., 1990; Eguiluz de Antuñano, 2001; González-Naranjo et al., 2008). Nomenclature of Jurassic and lowermost Cretaceous units adjacent to the Coahuila block varies because of the abrupt facies changes and limited exposure (Fig. 9).

Because Jurassic and Cretaceous strata around the edges of the Coahuila block consist of sediment derived directly from the block, samples of these strata provide insight into detrital-zircon provenance of this part of the Coahuila terrane (Fig. 8). Here (Figs. 1 and 8–11), we present sandstone petrography and previously unpublished results of detrital-zircon analyses from the northern flank and southeastern corner of the Coahuila block, as well as previously published results from the southwestern corner of the Coahuila block (Lawton and Molina-Garza, 2014) and from Potrero de Menchaca, northeast of the Coahuila block (Gray et al., 2008).

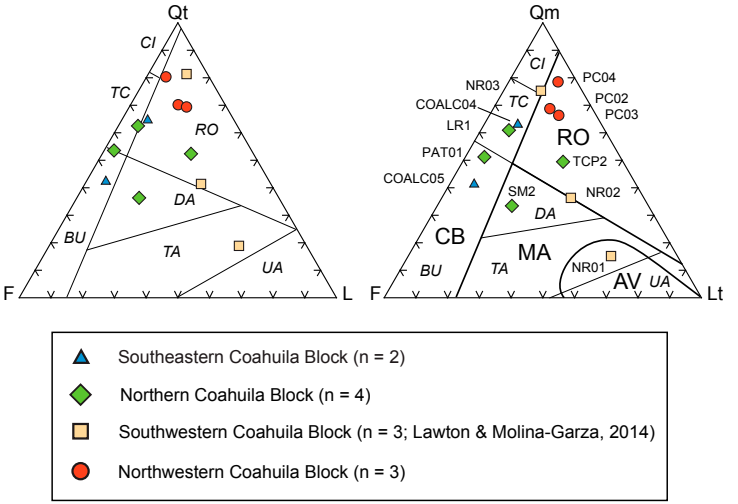

Figure 10. Detrital modes of Upper Jurassic–Lower Cretaceous sandstones deposited adjacent to Coahuila block. Provenance fields of QtFL (see Table 1 for definitions of grain categories) ternary plot after Dickinson (1985): magmatic arc provenance includes DA—dissected arc, TA—transitional arc, UA—undissected arc; continental block provenance includes CI—craton interior, TC—transitional continental, BU—basement uplift; RO—recycled orogen. Provenance fields of QmFLt (see Table 1 for definitions of grain categories) ternary plot modified after Dickinson (1985) by Garzanti (2016): CB—continental block; AV—anorogenic volcanic; MA—magmatic arc; RO—recycled orogen (or axial belt). Alphanumeric labels indicate samples in Table 1. Grain categories are defined in Table 1.

Petrography of Sandstones around the Coahuila Block

Samples were collected for petrography and U-Pb analysis from Upper Jurassic and lowermost Cretaceous strata deposited adjacent to the Coahuila block. Sites are adjacent to the northern, northwestern, southeastern, and southwestern parts of the block (Figs. 8 and 10; Table 1). The samples generally range from feldspathoquartzose plutoniclastic to lithoquartzose metamorphiclastic sandstone (classification of Garzanti, 2016). Samples stained for potassium feldspar were point-counted using the Gazzi-Dickinson counting technique (e.g., Ingersoll et al., 1984), which assigns most sand-sized crystal domains in plutonic rock fragments to monocrystalline grain categories (Qm, P, K [see Table 1 for definitions of grain categories]). Sandstone samples from the northern and southeastern flanks of the block are typically feldspar-rich (QtFL%F ranging 19%–44% and 27%–52%, respectively; Table 1 [see table for definitions of grain categories]) and are somewhat more quartzose, but with more metamorphic lithic fragments ranging from low to high metamorphic grade in Potrero Colorado (QtFL%L ranging 3%–28%; Table 1). Two samples derived from the southwestern part of the block are quartzofeldspatholithic volcaniclastic sandstones (Lawton and Molina-Garza, 2014) that plot in the magmatic arc provenance field on the QtFL ternary plot and transitional and dissected arc fields of Dickinson (1985) or anorogenic volcanic field of Garzanti (2016) on the QmFLt (see Table 1 for definitions of grain categories) ternary plot (Fig. 10). The observed sandstone compositions are compatible with moderate to extensive unroofing of continental basement in an extensional tectonic setting, either rifted or pull-apart (e.g., Garzanti, 2016). A general paucity of sedimentary lithic grains indicates limited exposure of sedimentary strata on the Coahuila block by the end of the Jurassic. The volcaniclastic samples adjacent to the southwestern edge of the block were previously interpreted to be a result of unroofing of a Middle Jurassic volcanic and sedimentary section that directly overlay crystalline basement of the block (Lawton and Molina-Garza, 2014). In summary, most samples are rich in unstable grains including feldspar, volcanic lithic fragments, and metamorphic lithic fragments, which likely represent first-cycle detritus rather than extensive recycling of older sedimentary rocks.

The inferred Late Triassic central Texas uplift (figure 1 *in* Dickinson et al., 2010) supplied detritus to the Chinle-Dockum fluvial system to the west and the Potosí fan to the south via the postulated El Alamar paleoriver east of the Coahuila block. The interpreted extent of the central Texas source terrain included parts of the Ouachita-Marathon thrust belt and Fort Worth foreland basin, in which the Pennsylvanian detrital-zircon populations (Alsalem et al., 2018) are similar to those in the Marathon foreland (Fig. 4). Some of the Triassic

TABLE 1. RECALCULATED MODAL POINT-COUNT DATA FOR COAHUILA BLOCK SANDSTONES, MEXICO

Sample	Formation	QtFL%			QmFLt%			LmLvLs%			QmPK%		
		Qt	F	L	Qm	F	Lt	Lm	Lv	Ls	Qm	P	K
Northern Coahuila block													
PAT01	Patula	54	43	3	51	43	6	NA	NA	NA	54	8	38
SM2	San Marcos	37	44	20	33	44	24	27	59	14	43	42	15
TCP2	Tanque Cuatro Palmas	53	19	28	49	19	32	49	48	3	72	16	13
LR1	Sierra El Granizo beds	63	31	6	61	31	9	NA	NA	NA	66	23	11
Northwestern Coahuila block (Potrero Colorado)													
PC02	San Marcos	71	14	15	68	14	18	NA	NA	NA	83	5	12
PC03	Eolian Colorado beds	70	12	18	66	12	22	NA	NA	NA	85	2	13
PC04	Fluvial Colorado beds	83	6	12	79	6	16	NA	NA	NA	93	2	4
Southeastern Coahuila block (Cañon Los Chorros)													
COALC04	La Casita	66	27	8	63	27	11	NA	NA	NA	70	14	15
COALC05	La Casita	43	52	6	41	52	8	NA	NA	NA	44	25	31
Southwestern Coahuila block (Lawton and Molina-Garza, 2014)													
08NR02	Carbonera	41	21	36	36	23	41	3	92	5	62	17	21
08NR03	La Casita	81	13	6	75	13	12	NA	NA	NA	86	1	13
08NR01	La Casita	19	21	60	15	21	64	0	100	0	42	33	25
X		57	25	18	53	25	22	20	75	6	67	16	18
SD		19	15	16	19	14	17	23	25	6	18	13	10

Notes: Qt—total quartz (= monocrystalline quartz [Qm] + polycrystalline quartz [Qp]); rare chert is included in Qp grain category. F—total feldspar (= alkali feldspar [K] + plagioclase [P]). Lt—total lithic fragments (= microcrystalline lithic fragments [L] + Qp). Lm—metamorphic lithic fragments; Ls—sedimentary lithic fragments; Lv—volcanic lithic fragments. NA—not calculated for samples with QtFL%L <20%; X—mean; SD—standard deviation.

sediment might have spread onto the Coahuila terrane and subsequently contributed to Jurassic–Cretaceous recycling; however, the lack of preserved Triassic sedimentary strata on the Coahuila terrane precludes direct evidence of a source for recycling. Petrographic data indicate that Jurassic–Cretaceous siliciclastic deposits derived from the Coahuila terrane (Fig. 10) consist largely of proximal, first-cycle sediment that is not consistent with recycling from a Triassic sedimentary succession. Alternatively, the similarity of detrital-zircon populations in the Marathon foreland (Fig. 4) to those in the Chinle-Dockum fluvial system (Dickinson et al., 2010) may indicate that the Marathon orogen (thrust belt and accreted Coahuila terrane) might have been the source for sediment delivered cratonward into the Chinle-Dockum system.

Detrital-Zircon Data from Sandstones around the Coahuila Block

Sampled strata include Upper Jurassic–Lower Cretaceous marginal-marine and fluvial strata at Sierra El Granizo, Valle San Marcos, and La Gavia anticline (Figs. 8, 9, and 11A); eolian and fluvial strata at Potrero Colorado adjacent to the northwestern part of the Coahuila block (Figs. 8, 9, and 11B); Upper Jurassic marginal-marine strata of La Casita Formation near the southeastern plunge end of the block (Figs. 8, 9, and 11C); and fluvial and marginal-marine strata in Cerros Coloraditos on the Rio Nazas near the southwest corner of the block (Figs. 8, 9, and 11D) (Lawton and Molina-Garza, 2014). Shallow-marine strata of the lowermost Cretaceous (Berriasian) Menchaca Formation were sampled at Potrero de Menchaca (Figs. 1 and 11A) (Gray et al., 2008).

Beds at Sierra El Granizo (Sample LR-1, Northern Coahuila Block)

Within the informally termed "lechas rojas" coarse-grained facies of inferred Late Jurassic age, a sandstone interbedded with granite-clast conglomerate was sampled (LR-1) on the north flank of Sierra El Granizo, on the southwestern flank of Valle San Marcos (Figs. 8 and 9). The abundance of granite clasts indicates that the drainage basin was underlain by extensive granitic intrusions, and the sample is dominated by Late Permian and Mesozoic grains ranging from 259 Ma to 180 Ma with a prominent age peak at 252 Ma (Fig. 11A). A single young grain at 153 ± 5 Ma is consistent with a latest Jurassic–earliest Cretaceous depositional age. The sample contains three late Paleozoic grains (329–283 Ma), two Sunsás-Oaxaquia grains, and a single Paleoproterozoic grain (ca. 2464 Ma).

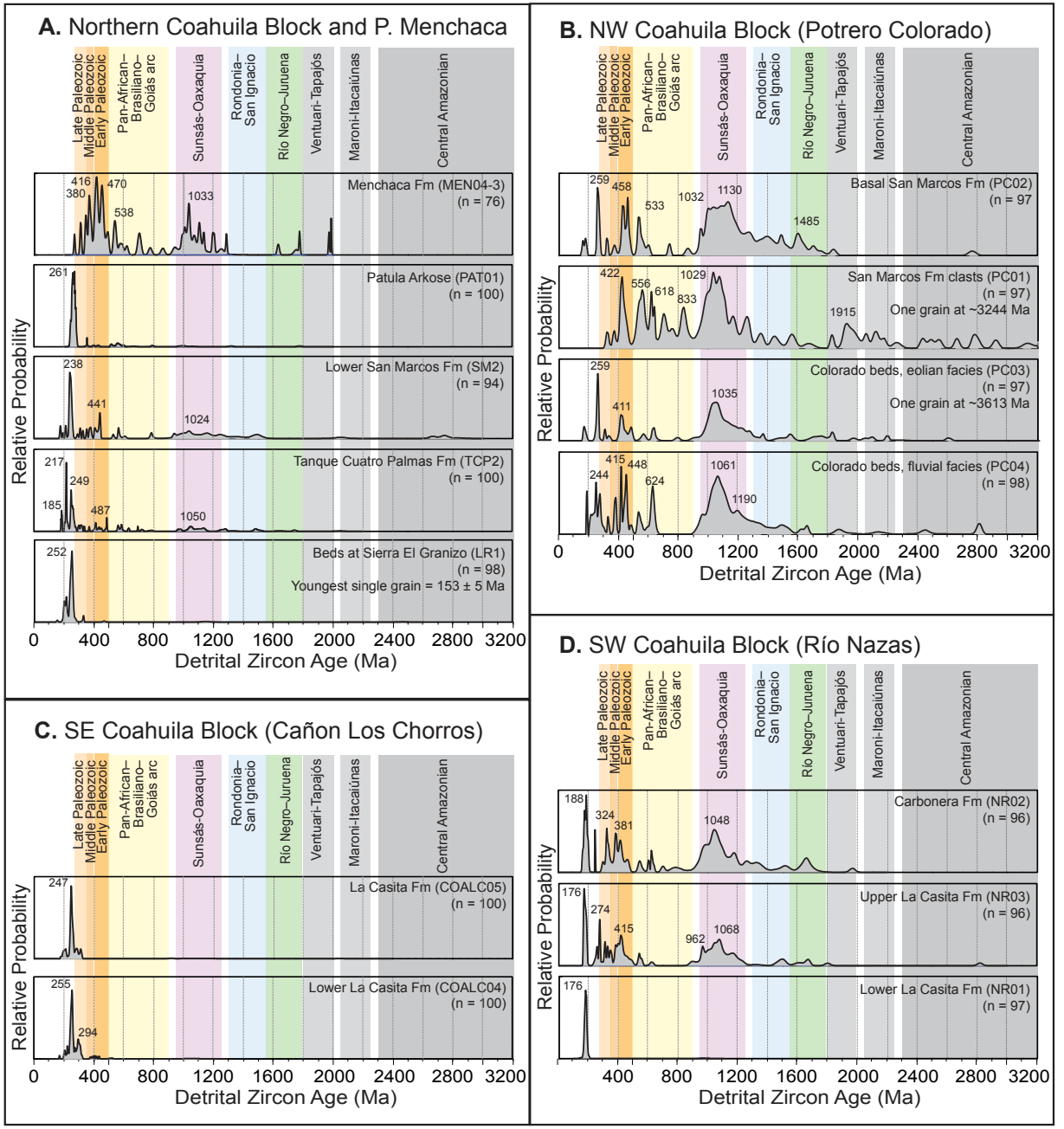

Figure 11. Relative U-Pb age-probability plots showing results from analyses of Mesozoic sandstones in Coahuila with respect to potential provenance provinces in the Coahuila terrane and Amazonia/Gondwana (age ranges shown by vertical color bands as in Fig. 4). Analytical data and location information are in Supplemental Tables S3, S4, and S5 (see text footnotes 3–5). Locations of sample sites are shown in Figure 8.

Tanque Cuatro Palmas Formation (Sample TCP2, Northern Coahuila Block)

The Upper Jurassic Tanque Cuatro Palmas Formation adjacent to Valle San Marcos (Figs. 8 and 9) was sampled from a shoreface sandstone in the upper part of the formation. The sample is dominated by Mesozoic grains (Fig. 11A). The older (pre–275 Ma) age fraction (n = 50) contains abundant grains of the Sunsás-Oaxaquia group (ca. 1266 Ma to ca. 964 Ma; n = 16; 32%) with a peak at ca. 1050 Ma. Early Paleozoic grains are also common (ca. 488 Ma to ca. 392 Ma; n = 10; 20%) with an age peak at ca. 487 Ma. Late Paleozoic grains occupy the range ca. 338 Ma to ca. 272 Ma (n = 8; 16%), Pan-African grains fall in the range ca. 784 Ma to ca. 562 Ma (n = 9; 18%), and Rio Negro–Juruena grains fall in the range ca. 1504 Ma to ca. 1329 Ma (n = 4; 8%). Other designated age groups are represented by one or two grains or none at all.

Lower San Marcos Formation (Sample SM2, Northern Coahuila Block)

Lower Cretaceous fluvial strata of the San Marcos Formation consist of red sandstone in amalgamated channel complexes interbedded with red siltstone. Sample SM2, from the middle part of the formation near the northwestern end of Valle San Marcos (Figs. 8 and 9), has a suite of grain ages similar to that of the Tanque Cuatro Palmas sample (TCP2), with 61 pre–275 Ma grains (Fig. 11A). A dominant Sunsás-Oaxaquia age group (n = 25; 46%) ranges in age from ca. 1269 (±107) Ma to ca. 969 Ma with an age peak at ca. 1024 Ma. Succeeding grain abundances are early Paleozoic (ca. 530 Ma to ca. 404 Ma; n = 10; 16%) with an age peak at ca. 441 Ma, Rondonia–San Ignacio (ca. 1511 Ma to ca. 1284 Ma; n = 9; 15%), Central Amazonian (ca. 2834 Ma to ca. 2661 Ma; n = 6; 10%), Pan-African (ca. 790 Ma to ca. 565 Ma; n = 5; 8%), and late Paleozoic (ca. 351 Ma to ca. 292 Ma; n = 4; 7%). Other age categories are absent or contain only two grains (Moroni-Itacaiúnas). A sample from the upper part of the San Marcos Formation on the west flank of the San Marcos anticline yielded a somewhat similar grain distribution with abundant early Paleozoic grains, but only one Sunsás-Oaxaquia grain (Gray et al., 2008).

Patula Arkose (Sample PAT01, Northeastern Coahuila Block)

Late Paleozoic grains (ca. 355 Ma to ca. 275 Ma; n = 17; 53%) dominate a quartzofeldspathic sandstone from the Patula Arkose (Krutak, 1965), or upper part of the San Marcos Formation (Eguiluz de Antuñano, 2001), in La Gavia anticline (Figs. 8, 9, and 11A). The sample contains 32 pre–275 Ma grains (Fig. 11A). Twelve younger grains in the range 274–271 Ma overlap with 275 Ma at 2σ error, causing the dominant peak to be ca. 261 Ma; Middle Permian grains are quite common in the sample. Other represented age groups include Pan-African (ca. 793 Ma to ca. 556 Ma; n = 7; 22%), early Paleozoic (ca. 529 Ma to ca. 400 Ma; n = 4; 12%), Sunsás-Oaxaquia (ca. 1056 Ma to ca. 977 Ma; n = 3; 9%), and Rio Negro–Juruena (ca. 1777 Ma; n = 1).

Menchaca Formation (Sample MEN04–3; Gray et al., 2008)

A sample of shallow-marine strata of the lowermost Cretaceous (Berriasian) Menchaca Formation collected at Potrero de Menchaca northeast of the Coahuila block (Fig. 1), roughly equivalent to the lower part of the San Marcos Formation (Fig. 9), yielded an age distribution (Gray et al., 2008) different from that of the samples collected closer to the Coahuila block (Fig. 11A). The Menchaca Formation was likely derived from the separate La Mula Island (Jones et al., 1984), which lay less than 50 km to the northwest of the sample site. The sample contains 75 pre–275 Ma grains. Age groups represented in the sample include, in order of decreasing abundance, Sunsás-Oaxaquia (ca. 1252 Ma to ca. 979 Ma; n = 23; 31%), early Paleozoic (ca. 493 Ma to ca. 398 Ma; n = 22; 29%), Pan-African (ca. 859 Ma to ca. 533 Ma; n = 12; 16%), late Paleozoic (ca. 350 Ma to ca. 308 Ma; n = 5; 7%), and Rio Negro–Juruena (ca. 1775 Ma to ca. 1632 Ma; n = 3; 4%). Two grains represent the Ventuari-Tapajós age group, at ca. 1987 Ma and ca. 1972 Ma. The distinctive age distribution of the sample illustrates the heterogeneity of pre-Mesozoic rock types in the Coahuila terrane.

Colorado Beds, Fluvial Facies (Sample PC04, Northwestern Coahuila Block)

Pebbly sandstone with trough cross-beds and quartz pebbles in the lower part of the exposed Jurassic–Lower Cretaceous section at Potrero Colorado constitute deposits of ephemeral braided streams within the informally named "Colorado beds" (Figs. 8 and 9). The sample contains 86 pre–275 Ma grains (Fig. 11B). Significant age groups represented in the sample include, in order of decreasing abundance, Sunsás-Oaxaquia (ca. 1249 Ma to ca. 951 Ma; n = 43; 50%), Rondonia–San Ignacio (ca. 1530 Ma to ca. 1273 Ma; n = 11; 13%), early Paleozoic (ca. 529 Ma to ca. 414 Ma; n = 10; 12%), and Pan-African (ca. 926 Ma to ca. 534 Ma; n = 8; 9%). Other age groups are not represented or contain fewer than three grains.

Colorado Beds, Eolian Facies (Sample PC03, Northwestern Coahuila Block)

Sandstone with large-scale planar cross-beds in the lower part of the eolian facies of the Colorado beds at Potrero Colorado (Figs. 8 and 9) contains 87 pre–275 Ma grains (Fig. 11B). Grains of the Sunsás-Oaxaquia group dominate the sample (ca. 1247 Ma to ca. 983 Ma; n = 45; 52%). Other age groups represented in the sample include, in order of decreasing abundance, early Paleozoic (ca. 485 Ma to ca. 407 Ma; n = 9; 10%), Pan-African (ca. 902 Ma to ca. 563 Ma; n = 7; 8%), Rio Negro–Juruena (ca. 1771 Ma to ca. 1565 Ma; n = 6; 7%), Rondonia–San Ignacio (ca. 1505 Ma to ca. 1305 Ma; n = 5; 6%), and Moroni-Itacaiúnas (ca. 2270 Ma to ca. 2069 Ma; n = 4; 5%). One old grain at 3613 Ma is significantly older than the Central Amazonian age group.

Clasts in San Marcos Formation (Sample PC01, Northwestern Coahuila Block)

A sample of quartzite pebbles from the lowermost part of the San Marcos Formation at Potrero Colorado (Figs. 8 and 9), ranging in size from 1 to 5 cm in diameter, yielded the most diverse range of grain ages of the Coahuila block samples, including a wide range of Paleoproterozoic and Mesoproterozoic ages (Fig. 11B). Sunsás-Oaxaquia grains form the dominant age group (ca. 1247 Ma to ca. 976 Ma; $n = 34$; 36%) with a peak at ca. 1029 Ma. Pan-African grains form a significant age group (ca. 852 Ma to ca. 534 Ma; $n = 21$; 22%) with peaks at ca. 833 Ma, ca. 618 Ma, and ca. 556 Ma. Other important age groups include early Paleozoic grains (ca. 526 Ma to ca. 412 Ma; $n = 8$; 9%) with an age peak at ca. 422 Ma, Ventuari-Tapajós (ca. 2016 Ma to ca. 1824 Ma; $n = 7$; 7%) with an age peak at ca. 1915 Ma, Rondonia–San Ignacio (ca. 1564 Ma to ca. 1339 Ma; $n = 6$; 6%), Central Amazonian (ca. 3244 Ma to ca. 2658 Ma; $n = 6$; 6%), and Moroni-Itacaiúnas (ca. 2256 Ma to ca. 2053 Ma; $n = 5$; 5%). A single young grain at 316.5 ± 9.3 Ma suggests that the quartz arenite unit from which the pebbles were derived is at least as young as Early to Middle Pennsylvanian. The pebbles yield a characteristically Gondwanan detrital-zircon age distribution.

Basal San Marcos Formation (Sample PC02, Northwestern Coahuila Block)

A sample of fluvial sandstone from the lowermost part of the San Marcos Formation at Potrero Colorado (Figs. 8 and 9) contains 91 pre–275 Ma grains (Fig. 11B). The composition (Fig. 10) and texture indicate that the sandstone was likely derived from directly underlying unconsolidated eolian sediment. Sunsás-Oaxaquia grains dominate the sample (ca. 1270 Ma to ca. 945 Ma; $n = 46$; 51%) with age peaks near 1130 Ma and 1032 Ma. Other age groups represented in the sample include Rondonia–San Ignacio (ca. 1522 Ma to ca. 1279 Ma; $n = 15$; 16%) with an age peak of ca. 1485 Ma, early Paleozoic (ca. 530 Ma to ca. 420 Ma; $n = 10$; 11%) with an age peak near 458 Ma, Rio Negro–Juruena (ca. 1711 Ma to ca. 1590 Ma; $n = 8$; 9%), and Pan-African (ca. 861 Ma to ca. 533 Ma; $n = 7$; 7%). Other age groups are not represented or contain only one or two grains. An old grain at ca. 2763 Ma is older than the Central Amazonian age group.

La Casita Formation (Samples COALC04 and COALC05, Southeastern Coahuila Block)

Two quartzofeldspathic sandstone samples from coarse-grained shoreface deposits of the Upper Jurassic La Casita Formation in Cañon Los Chorros near the southeastern plunge end of the Coahuila block (Figs. 8 and 9) are similar in detrital-zircon characteristics (Fig. 11C). Permian and Triassic grains younger than 275 Ma dominate both samples, such that older grains constitute only 35% and 24%, respectively, of the samples COALC04 and COALC05 (Fig. 11C). Of the older grains, late Paleozoic grains are most abundant in both samples, including a peak near 294 Ma in COALC04. Subordinate grain ages include the early Paleozoic and Sunsás-Oaxaquia groups. The detrital-zircon age distribution of La Casita samples (Fig. 11C) is similar to that of the Patula Arkose (Fig. 11A). Similar results for La Casita Formation in Cañon Los Chorros were reported previously (Ocampo-Díaz et al., 2014).

La Casita Formation (Samples NR01, NR02, NR03, Southwestern Coahuila Block; Lawton and Molina-Garza, 2014)

Jurassic–Cretaceous fluvial and marginal-marine sandstones, now in an inverted basement graben within the Coahuila terrane in Cerros Coloraditos on the Rio Nazas (Figs. 8, 9, and 11D), had proximal sources in uplifted fault blocks, probably dominated by the Coahuila block, flanking the graben (Lawton and Molina-Garza, 2014). The stratigraphically lowest sample (NR01) has only one grain (965.2 ± 20.5 Ma) older than 275 Ma, indicating that Jurassic cover strata had not been unroofed from the Coahuila block. The other two, stratigraphically higher samples have a range of older ages, indicating basement contributions. Sample NR03 has 78 grains with ages older than 275 Ma; sample NR02 has 84 grains older than 275 Ma. The dominant concentration of detrital-zircon ages (NR03, $n = 38$, 49% and NR02, $n = 42$, 50%) is in the Sunsás-Oaxaquia group between 1277 Ma and 920 Ma with peaks at 1068 Ma and 1048 Ma in samples NR03 and NR02, respectively (Fig. 11D) (Lawton and Molina-Garza, 2014). The next greatest concentration of ages is the early Paleozoic group between 486 Ma and 379 Ma (NR03, $n = 17$, 22% and NR02, $n = 12$, 14%) with peaks at 415 Ma and 381 Ma in samples NR03 and NR02, respectively (Fig. 11D) (Lawton and Molina-Garza, 2014). The late Paleozoic group has ages between 350 Ma and 288 Ma (NR03, $n = 7$, 49% and NR02, $n = 7$, 50%) with peaks around 324 Ma in both samples (Fig. 11D) (Lawton and Molina-Garza, 2014). Lesser concentrations include Pan-African between 890 Ma and 534 Ma, Rondonia–San Ignacio between 1519 Ma and 1318 Ma, and Rio Negro–Juruena between 1799 Ma and 1563 Ma (Fig. 11D) (Lawton and Molina-Garza, 2014). Older single grains have ages equal to Ventuari-Tapajós (1964 Ma, NR02) and Central Amazonian (2819 Ma, NR03).

Summary of Detrital-Zircon Age Data from around the Coahuila Block

Samples from around the Coahuila block ($N = 13$; Fig. 11) constitute 1265 total analyses. Of these, one grain at ca. 111 Ma was eliminated because it is younger than the stratigraphically determined depositional age of the sample. The sample set, which does not include the Menchaca Formation sample analyzed in a different laboratory, is dominated by a continuous range of overlapping grain ages (at 2σ) ranging from 275 Ma to 148 Ma ($n = 525$ grains; 42% of the analyzed population). Because these ages are younger than 275 Ma, the approximate

inferred depositional age of the youngest sample from the Marathon foreland (Road Canyon Formation), they are not considered in the discussion of the possible provenance for Marathon detrital zircons; however, they are shown on the probability distribution plots of Figure 11. The detrital-zircon ages, ranging in age from 3613 Ma to 275 Ma (n = 739), provide a sample of age groups from the basement within the Coahuila terrane and, thus, potentially available for dispersal to the Marathon foreland. Each sample from the sandstones around the fault boundaries of the Coahuila block specifically characterizes the sedimentary detritus from the local basement and other rocks of the local drainage basin; however, other parts of the Coahuila terrane may differ somewhat from the relatively local samples of basement detritus. Considering the Gondwanan affinity of the Coahuila terrane, the detrital-zircon populations may be grouped according to provinces in Gondwana (Figs. 4 and 11).

Older Gondwanan age groups represent a subordinate fraction of the pre–275 Ma grain population. Grain percentages cited below represent fractions of the pre–275 Ma age population. The oldest grain group, Central Amazonian, represents 2.4% of the total population (n = 18) and ranges from 3244 Ma to 2629 Ma. One older grain is 3613 ± 35 Ma. The Moroni-Itacaiúnas age group contains 2% of the total grains with ages ranging from 2270 Ma to 2038 Ma. The Venturi-Tapajós age group contains 1.8% of the grain ages, ranging from 2016 Ma to 1824 Ma.

Late Paleoproterozoic to early Mesoproterozoic grains form a modest fraction of the grain age population. Grains with ages in the Rio Negro–Juruena age group compose 4.6% (n = 34) of the age population and range from 1799 Ma to 1564 Ma. Grains in the Rondonia–San Ignacio age group constitute 8.1% (n = 60) and range in age from 1549 Ma to 1283 Ma.

Grains of the Sunsás-Oaxaquia group constitute most pre-Triassic grain ages derived from the Coahuila block, making up 40.1% of the pre–275 Ma age population with an age range of 1273 ± 29 Ma to 937 ± 20 Ma. Grains with ages that correspond to the group of Pan-African–Brasiliano–Goiás arc constitute 10.7% of the population (n = 79) and range from 915 Ma to 530 Ma. Early Paleozoic grains constitute 11.5% of the population (n = 85) and range in age from 529 Ma to 400 Ma. Late Paleozoic grains make up 13.1% of the population (n = 97) and range in age from 355 Ma to 273 Ma.

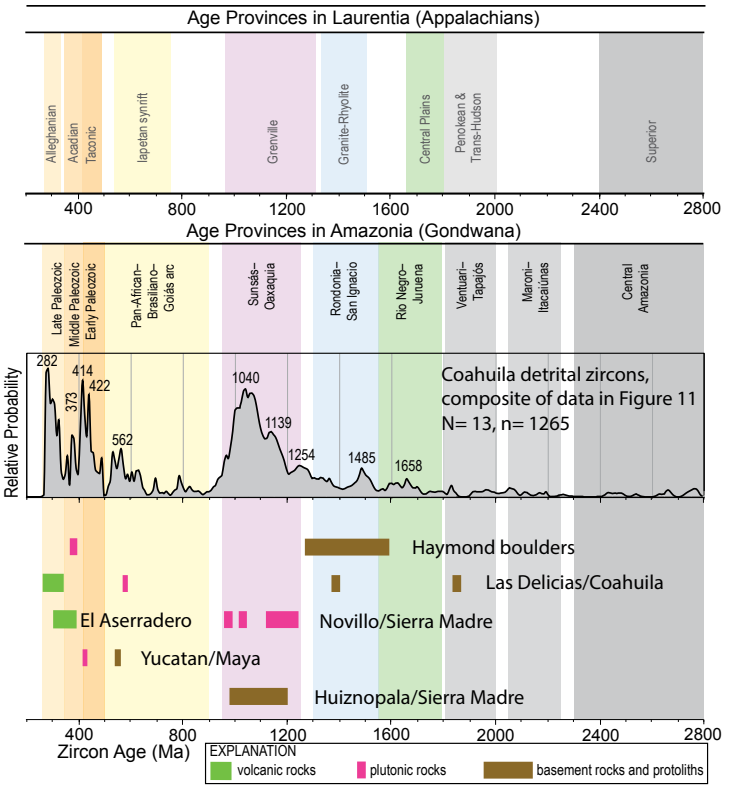

Figure 12. Diagram of ages of potential primary sources in Coahuila and nearby accreted terranes for detrital zircons in the Marathon foreland clastic-wedge sandstones. Colored horizontal bars indicate crystallization ages of volcanic and plutonic rocks, as well as xenocrysts, inclusions, and protoliths within the primary igneous rocks in Coahuila and nearby Gondwanan terranes (data from references cited in the text). Relative probability plot shows composite of U-Pb ages of detrital zircons from Mesozoic sandstones adjacent to the Coahuila block (compiled from data plotted in Fig. 11, except for sample MEN04–3, which is north of the block) to illustrate the range of detrital-zircon populations from proximal sources in Coahuila. Vertical colored bands show age brackets of potential provenance provinces in the Coahuila terrane and Amazonia/Gondwana and in Laurentia and the Appalachians (from Figs. 3 and 4).

Igneous Rocks in and around the Coahuila Terrane

In the western part of the Coahuila terrane, Las Delicias Formation (Fig. 8) includes deep-water bouldery conglomeratic mass-gravity sediment-flow deposits (McKee et al., 1999), indicating deposition in intra-arc or arc-flank basins (Dickinson and Lawton, 2001). The boulders include granitoid rocks derived from the basement of the Coahuila block with U-Pb intercept ages between 1232 ± 7 Ma and 1214 ± 2 Ma (Fig. 12) (Lopez et al., 2001). A well-defined upper-intercept age of 1851 ± 80 Ma on a single clast was interpreted to indicate an inherited basement component (Fig. 12) (Lopez et al., 2001). One granite boulder yielded a concordia intercept age of 580 ± 4 Ma on the basis of four abraded grain fractions. This interpreted crystallization age documents Pan-African magmatism in the Coahuila block (Fig. 12); an Nd model age of ca. 1394 Ma indicates assimilation of older crust (Lopez et al., 2001).

Dated samples of Las Delicias magmatic arc (Fig. 8) include in situ volcanic rocks, volcanic blocks in sediment-gravity flows, and a plutonic rock (Lopez, 1997). In situ volcanic rocks are represented by La Pesúna peperite with a concordant zircon U-Pb age of 331 ± 4 Ma (Middle-Late Mississippian boundary) and a dacitic ignimbrite with a concordant U-Pb age of 303 ± 13 Ma (Late

Pennsylvanian); allochthonous volcanic blocks include two dacite ignimbrites with U-Pb intercept ages of ca. 300 Ma and ca. 270 Ma (Late Pennsylvanian and Middle Permian); a plutonic sample from the foot of Sierra El Granizo (Fig. 8) yielded a concordant grain fraction with a U-Pb age of 285 ± 3 Ma (Early Permian). The documented age range of Las Delicias arc in the Coahuila block is thus ca. 331 Ma to ca. 270 Ma (Fig. 12) (Late Mississippian to early Guadalupian; Lopez, 1997). This age range is represented by 127 grains (10%) of the detrital-zircon sample set, including all grains for which the 2σ error in age is within the age bracket. Other volcanic arc components have U-Pb zircon ages of 303 ± 5 Ma and 268 ± 6 Ma (Fig. 12) (Lopez, 1997; Stewart et al., 1999; Poole et al., 2005). Younger granitoid plutons with U-Pb zircon ages of 236–222 Ma, ages that are well represented in the Coahuila block detrital-zircon U-Pb ages, indicate post-Marathon phases of magmatism (Poole et al., 2005).

South of the recognized Coahuila terrane, the Sierra Madre terrane (Fig. 1) may be a separate Gondwanan terrane (Stewart et al., 1999); however, along with Coahuila, the Sierra Madre terrane is generally considered to be part of the larger Oaxaquia terrane (Ortega-Gutierrez et al., 1995; Lawlor et al., 1999). The Sierra Madre terrane, near Ciudad Victoria, includes the Novillo Gneiss (Fig. 1) (Stewart et al., 1999), a granulite-facies complex that is intruded by two gabbro-anorthosite suites with U-Pb zircon ages of 1235–1115 Ma and 1035–1010 Ma, as well as a late anorthosite pegmatite with an age of 978 ± 13 Ma (Fig. 12) (Cameron et al., 2004). In a concordia plot, a discordant array of U-Pb zircon ages from El Asseradero Rhyolite (Fig. 1) has a lower intercept at 334 ± 39 Ma, which is interpreted to be the age of crystallization (Fig. 12) (Stewart et al., 1999). An upper intercept at 1086 ± 94 Ma is interpreted to be the age of basement rocks (Fig. 12) that were incorporated into the arc magma. Farther south in the Sierra Madre terrane, U-Pb zircon ages of orthogneiss, anorthosite, metatonalite, and postdeformational pegmatite from the Huiznopala Gneiss of the basement at Molango, Hidalgo, Mexico, range in age from 1203 ± 1 Ma to 987 ± 1 Ma; ages of dominant early magmatism range from 1203 ± 1 Ma to 1007 ± 3 Ma (Figs. 1 and 12) (Lawlor et al., 1999).

Farther outboard, the Yucatan block in the Maya terrane (Fig. 1), which may or may not be part of the same terrane as Coahuila, has basement rocks with a U-Pb zircon age of 554 ± 5 Ma and a younger rock with a U-Pb zircon age of 418 ± 6 Ma (Fig. 12) (Krogh et al., 1993). Different phases of a pluton in the Maya Mountains of Belize yielded U-Pb intercept ages of 418 ± 4 Ma and 404 ± 3 Ma (Steiner and Walker, 1996), and rhyolite interbedded in conglomerate yielded a U-Pb median age of 406 +7/–6 Ma (Martens et al., 2010). The present location of the Yucatan block is a result of rotation away from south Texas during Mesozoic opening of the Gulf of Mexico (Pindell and Kennan, 2009), indicating a late Paleozoic palinspastic location to the east of the Coahuila terrane.

These available data indicate that Coahuila is a Gondwanan terrane with middle to late Mesoproterozoic basement overprinted by Pan-African orogenesis and magmatism (Fig. 12) (Lopez et al., 2001; Poole et al., 2005). The late Paleozoic Las Delicias arc (331 ± 4 Ma to 269 ± 6 Ma) is consistent with a continental-margin arc along the leading edge of the Gondwanan Coahuila microcontinental terrane, beneath which Laurentian oceanic crust was subducted southward during the time of Early Mississippian to Early Permian deposition of synorogenic clastic sediment in the Marathon foreland. Incorporation of the Coahuila terrane into the hinterland of the Marathon orogen provided a source of Mesoproterozoic, Neoproterozoic, and Paleozoic detrital zircons (Fig. 12) for dispersal into the Marathon foreland.

Coahuila Provenance for Marathon Foreland

The distributions of detrital-zircon ages from the Marathon foreland have specific counterparts in the Coahuila terrane, indicating a good match for the provenance (Figs. 4 and 12). The youngest cluster of ages (495–280 Ma; Fig. 4) corresponds to a detrital-zircon concentration in Coahuila sandstones (Figs. 11 and 12), as well as to igneous rocks in Coahuila, Sierra Madre, and Yucatan (Fig. 12). Prominent concentrations of ages between 745 Ma and 500 Ma (Fig. 4) correspond in age to Pan-African components of Gondwanan accreted terranes, which are represented by igneous rocks and detrital zircons in Coahuila (Fig. 12). A strong to dominant peak (1150–907 Ma; Fig. 4) matches the age of the Sunsás province of Amazonia/Gondwana (Fig. 12). A generally consistent, but secondary, scatter of ages and minor peaks between 2050 Ma and 1150 Ma span the ages of Ventuari-Tapajós, Rio Negro–Juruena, and Rondonia–San Ignacio components of the Amazonia craton of Gondwana (Figs. 4, 11, and 12). An older grouping of ages (3490–2379 Ma) corresponds in age to the Central Amazonian craton. In summary, all of the ages of detrital zircons in the Marathon foreland have potential sources in the Coahuila terrane (Fig. 12).

SEDIMENT DISPERSAL ONTO THE SOUTHERN LAURENTIAN CRATON

Delaware Intracratonic Basin

The Delaware intracratonic basin is inboard from the apex of the Marathon salient of the thrust belt (Fig. 1), and the sedimentary fill of the Delaware basin provides samples of sediment dispersal onto the southern part of the Laurentian craton. Middle Permian sandstones in the Delaware basin have detrital-zircon populations (Soreghan and Soreghan, 2013; Xie et al., 2018) that are similar to those in the Marathon foreland, but some differences are evident (Fig. 13). All of the samples have peaks between 1200 Ma and 1000 Ma. Most, but not all, samples from the Delaware basin have concentrations of Pan-African ages and relatively abundant ages in the range of 1800–1300 Ma. The sandstones contain late Paleozoic grains but not as abundantly as in the Marathon samples, and the age range of 2200–1800 Ma is more sparsely represented in the Delaware basin (Fig. 13). Although previous interpretations have proposed a source in the Ancestral Rockies for the Delaware basin fill, the detrital-zircon data indicate an ultimate source in the Marathon orogen, including Gondwanan accreted terranes, mixed with detritus from other, more

distant sources (Soreghan and Soreghan, 2013). In detail, the stratigraphically lower Brushy Canyon Formation (Fig. 2) has a relatively narrow peak of early–middle Paleozoic grains, minor Pan-African components, and a dominant Mesoproterozoic peak (Fig. 13), which have been interpreted to reflect somewhat mixed and recycled detritus (Soreghan and Soreghan, 2013), possibly fed by a continental-scale river from the Appalachians (Xie et al., 2018). Stratigraphically upward in the Cherry Canyon and Bell Canyon Formations (Fig. 2), the detrital-zircon populations include a wider range of early to late Paleozoic grains, a substantial Pan-African peak, and a correspondingly reduced Mesoproterozoic peak (Fig. 13) (Soreghan and Soreghan, 2013; Xie et al., 2018), all suggesting a dominant concentration of detritus from Coahuila (Fig. 12). The Brushy Canyon samples (Soreghan and Soreghan, 2013; Xie et al., 2018) are very similar (Kolmogorov-Smirnov [K-S] $P = 0.992$, $D = 0.044$) to each other, as are the Bell Canyon and Cherry Canyon samples (K-S $P = 0.345$, $D = 0.086$). The Bell Canyon samples of Soreghan and Soreghan (2013) are somewhat similar (K-S $P = 0.262$, $D = 0.107$) to their Brushy Canyon samples, but less similar (K-S $P = 0.088$, $D = 0.128$) to Brushy Canyon samples of Xie et al. (2018). Bell Canyon and Cherry Canyon samples (Xie et al., 2018) are unlike (K-S $P = 0.047$, $D = 0.125$ and $P = 0.034$, $D = 0.125$) either of the Brushy Canyon samples. The combined data support the interpretations (Soreghan and Soreghan, 2013; Xie et al., 2018) of a change through time in provenance of sediment dispersal into the Delaware basin. Comparisons of detrital-zircon populations in Permian sandstones in the Delaware basin with those in the Marathon foreland (Fig. 13) generally support an interpretation of fluvial dispersal of detritus onto the craton from the Marathon orogen and accreted Gondwanan terranes, followed by eolian redistribution of sediment from the broad foreland and southern craton to the Delaware basin (Soreghan and Soreghan, 2013). In contrast, K-S test results ($P = 0.000$ to 0.019, $D = 0.171$ to 0.125) indicate that the Delaware and Marathon populations are likely from different source terranes.

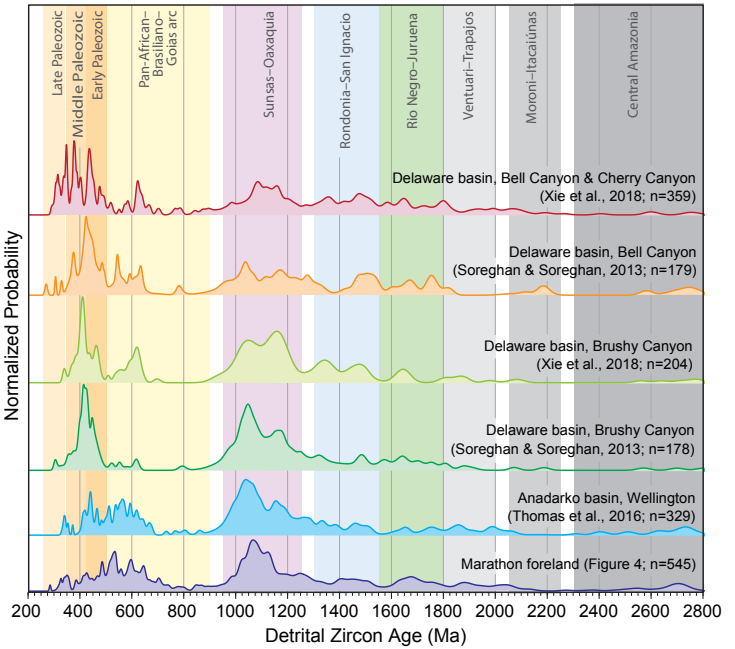

Figure 13. Composite relative probability plot of U-Pb ages of detrital zircons from four sandstones in the Marathon foreland (data from Fig. 4), a relative probability plot of U-Pb ages of a sample from the Lower Permian Wellington Formation on the Arbuckle uplift in the proximal part of the Anadarko basin (from Thomas et al., 2016), and four composite relative probability plots of U-Pb ages of detrital zircons from sandstones in the lower and upper parts of the Permian Delaware Mountain Group (DMG, Fig. 2) in the Delaware basin (from Soreghan and Soreghan, 2013; Xie et al., 2018). Vertical colored bands show age brackets of potential provenance provinces in the Coahuila terrane and Amazonia/Gondwana (from Fig. 4).

Anadarko Intracratonic Basin and Arbuckle-Wichita Uplifts

The Anadarko basin is more distal from the Marathon thrust front than is the Delaware basin and is an important depositional basin on the southern part of the Laurentian craton (Fig. 1). The Arbuckle and Wichita basement uplifts within the late Paleozoic Southern Oklahoma fault system form the southern boundary of the Anadarko basin. The initial and most proximal late Paleozoic sedimentary accumulations unconformably overlap eroded Paleozoic sedimentary rocks, Cambrian synrift rocks, and Precambrian basement rocks (Thomas et al., 2016). Local detritus dominates the proximal deposits, which include first-cycle zircons from the 535 Ma Wichita Granite Group, as well as recycled grains with ages older than 2400 Ma from lower Paleozoic sandstones (Thomas et al., 2016). A few meters stratigraphically above the proximal deposits, the sandstones have a completely different population of detrital zircons, indicating sediment from sources other than the local ones. Detrital zircons from the Lower Permian Wellington Formation have two dominant groups of U-Pb ages: 1340–960 Ma with peaks at 1326, 1151, and 1040 Ma; and 673–329 Ma with peaks at 563, 437, and 339 Ma (Fig. 13). The εHf_t values for 600–500 Ma grains in the Wellington Formation are more negative than those from the Wichita Granite, indicating a source other than the local synrift igneous rocks (Thomas et al., 2016). The groupings generally are similar to those in the Marathon foreland, suggesting that dispersal of sediment spread across the southern craton from Marathon to the Anadarko basin. A K-S test ($P = 0.470$, $D = 0.059$) indicates that the Wellington and Marathon populations are likely not from different source terranes.

DISCUSSION OF PROVENANCE FOR SEDIMENTS IN THE MARATHON FORELAND

Some of the detrital-zircon ages from the Marathon foreland uniquely represent accreted Gondwanan terranes (Fig. 4); however, because of overlap

between Laurentian and Gondwanan ages, zircons of some ages have been interpreted to be from sources in Laurentia, especially the Appalachians (e.g., Gleason et al., 2007; Soreghan and Soreghan, 2013). Various interpretations of continent-scale dispersal range from fluvial systems along the orogenic foreland to turbidite fans in remnant ocean basins along the length of the Appalachian-Ouachita-Marathon orogen (e.g., Graham et al., 1976; Gleason et al., 1994, 2007; Xie et al., 2018). All of these interpretations involve an ultimate sediment source in the Appalachians with possibly some subregional recycling; therefore, a comparison of Marathon (the ultimate sink) detrital-zircon populations with those in the Appalachian foreland (the ultimate source) provides an evaluation of provenance. A composite of the Marathon data reported here shows some significant differences from a composite plot of detrital-zircon data from Mississippian–Permian sandstones in the Appalachian foreland (Fig. 14) (Thomas et al., 2017). A K-S test ($P = 0.000$, $D = 0.164$) indicates that the Appalachian and Marathon populations are significantly different and are likely not from the same source terranes.

Synorogenic Alleghanian-age plutons are well known in the Appalachian internides; however, synorogenic zircons with ages of the Alleghanian orogen (330–270 Ma) are very rare (7 grains of 3564; Thomas et al., 2017) in sandstones of the Appalachian foreland (Fig. 14). In contrast, grains of that age range are more abundant in the Marathon foreland (Fig. 4), where local sources were available among the late Paleozoic arc-magmatic rocks of the Coahuila terrane (Fig. 12). Synorogenic zircons with Taconic and Acadian ages (490–350 Ma) have similar abundances in the Marathon and Appalachian forelands, and potential primary sources were available in the internides of both systems. For zircons in the age range of 500–400 Ma, εHf_t values in both Laurentia and Amazonia have a wide range; however, εHf_t peak density in the Marathon foreland closely matches the greatest concentration in Amazonia and contrasts with that in the Appalachians (Fig. 7B).

Zircons with ages of 800–500 Ma, representing Pan-African–Brasiliano–Goiás arc (Gondwanan) accreted terranes, are present but not abundant in the Appalachian foreland; however, grains with those ages are an important component of the Marathon foreland population, forming one of the most prominent probability peaks (Fig. 14). Grains of this age range are also abundant in sand derived from the Coahuila block (Fig. 11). The abundance of Pan-African grains in the Marathon foreland strongly contrasts with the Appalachian populations. More generally, Gondwanan terranes show more igneous activity than the Appalachian orogen during the time 800–500 Ma (Fig. 7). Another alternative for a source of zircons with ages of 765–530 Ma is lapetan synrift igneous rocks along the rifted margin of Laurentia, particularly the synrift igneous rocks (539–530 Ma) in the Wichita and Arbuckle uplifts along the Southern Oklahoma fault system (Fig. 1) (e.g., Gleason et al., 2007; Soreghan and Soreghan, 2013). Detrital zircons from lapetan synrift rocks cannot be distinguished from Pan-African igneous rocks on the basis of age alone; however, εHf_t values offer a discriminant (Thomas et al., 2016). Detrital zircons with ages of ca. 535 Ma constitute the proximal detritus from synrift granite in the Wichita uplift; positive εHf_t values of +4.7 to +10.1 (Fig. 7) indicate juvenile

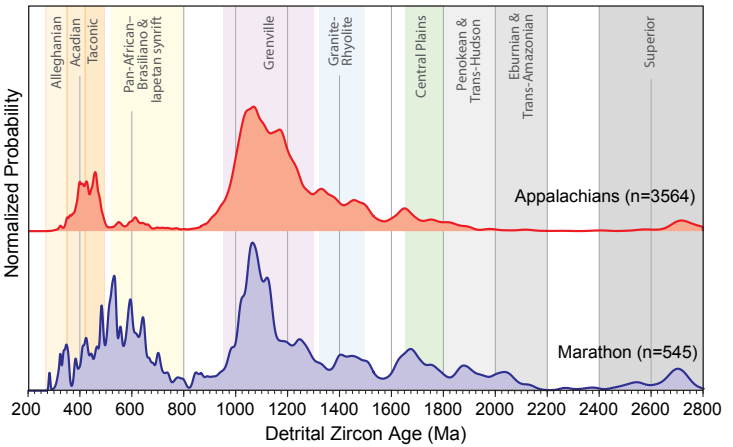

Figure 14. Comparison of a composite relative probability plot of U-Pb ages of detrital zircons from four sandstones in the Marathon foreland (data from Fig. 3) with a composite relative probability plot of U-Pb ages of detrital zircons from 29 sandstones in the Appalachian foreland (from Thomas et al., 2017). Vertical colored bands show age brackets of potential provenance provinces in Laurentia and the Appalachians (from Fig. 3).

magmas, consistent with petrographic data. In contrast, the detrital zircons in the age range of 800–500 Ma in the Marathon foreland have εHf_t values of +8.5 to −27.3 (Figs. 4 and 7), indicating assimilation of older continental crust, which is consistent with other isotopic data for Coahuila igneous rocks. In addition, the igneous rocks along the Southern Oklahoma fault system were covered by onlap of Early Permian strata and were not available to supply sediment to regional dispersal after that time (Soreghan and Soreghan, 2013).

Mesoproterozoic detrital zircons generally dominate the samples in both the Marathon foreland and Appalachians (Fig. 14). For the Appalachian foreland, the provenance is interpreted to be rocks of Grenville age within the orogen (Thomas et al., 2017). Rocks of the same age in the Sunsás province cannot be distinguished from other "Grenville" rocks on the basis of age, and a Sunsás age constitutes the dominant peak in sedimentary detritus in Coahuila (Fig. 11) (Lawton and Molina-Garza, 2014). For zircon grains older than 900 Ma, εHf_t values in the Appalachians are dominantly positive, although a few are negative (Fig. 7). In contrast, εHf_t values for zircons in Amazonia have a larger range than the Appalachian zircons, including more negative values (Fig. 7). In general, the Appalachian and Amazonia data strongly overlap in the range of positive values; however, the Amazonia data include more abundant points in the more negative range (Fig. 7). In the context of the regional distributions, the εHf_t data from Marathon sandstones are most concentrated in the range of overlap of the Appalachian and Amazonia εHf_t values; however, Marathon values also extend into the more negative range, which is more characteristic of Amazonia than the Appalachians (Fig. 7), indicating affinity of the Marathon detrital zircons with a source in Gondwanan accreted terranes.

In the Appalachian foreland, zircons in the age range of 2200–1350 Ma generally decrease in abundance with increase in age (Fig. 14). These zircon grains ultimately have sources in North American Midcontinent Precambrian provinces, as well as Trans-Amazonian (Gondwanan) accreted terranes (Thomas et al., 2017). The sediment supply to the late Paleozoic Appalachian foreland included recycling from synrift and passive-margin sedimentary deposits, enclaves of older provinces within the Grenville province, and accreted Gondwanan terranes (Thomas et al., 2017). The general decrease in abundance with increase in age in the Appalachian foreland contrasts with a generally moderate but more relatively uniform abundance of detrital zircons through the age range of 2200–1350 Ma in the Marathon foreland sandstones (Figs. 3, 4, and 14). Potential sources, represented by igneous rocks and detrital zircons, correspond to Ventuari-Tapajós, Rio Negro–Juruena, and Rondonia–San Ignacio components of the Amazonia craton of Gondwana (Fig. 4); the Marathon samples differ from the Appalachian populations in relative abundance of these older grains (Fig. 14).

Relatively rare older detrital zircons in the Appalachian foreland have ages (2950–2530 Ma) that correspond to the Superior province of interior Laurentia (Fig. 14) and are interpreted to have been supplied to the late Paleozoic foreland through recycling from synrift and passive-margin sedimentary rocks in the Appalachian orogen (Thomas et al., 2017). Zircons of the same age range were available from the Central Amazonia province of Gondwana (Figs. 4 and 12), and zircons of that age are about as abundant in the Marathon foreland as in the Appalachian foreland (Fig. 14).

CONCLUSIONS

Although the Marathon detrital-zircon populations are broadly comparable to those in the Appalachian foreland, some Marathon components differ distinctly from the Appalachians (Fig. 14). All of the Marathon components that are more abundant than equivalent ages in the Appalachian foreland have potential sources in the Coahuila terrane or nearby accreted Gondwanan terranes. The Marathon components that are similar in abundance to the Appalachian populations also have potential sources in Coahuila. Thus, Coahuila provides sources for all of the detritus analyzed from the Marathon foreland. The match of ages of the Marathon detritus and of the Coahuila terrane requires no other distant provenance or mixing from other sources such as the Appalachians. All of the detrital zircons in Middle Pennsylvanian to Middle Permian sandstones in the Marathon foreland could have come from the accreted Coahuila (Gondwanan) terrane in the interior of the Marathon orogenic belt.

Dispersal of detritus from Coahuila into the Marathon foreland and ultimately onto the southern craton of Laurentia evolved along with the Marathon orogen and accretion of the Coahuila terrane to the southern margin of Laurentia (Fig. 15). A thick accumulation of dark-colored, mud-dominated sediment of the Mississippian Tesnus Formation records an abrupt increase in the rate of siliciclastic deposition, consistent with the initiation of orogenic sources of sediment (Fig. 15). The depositional age of tuff in the Tesnus Formation is equal to that

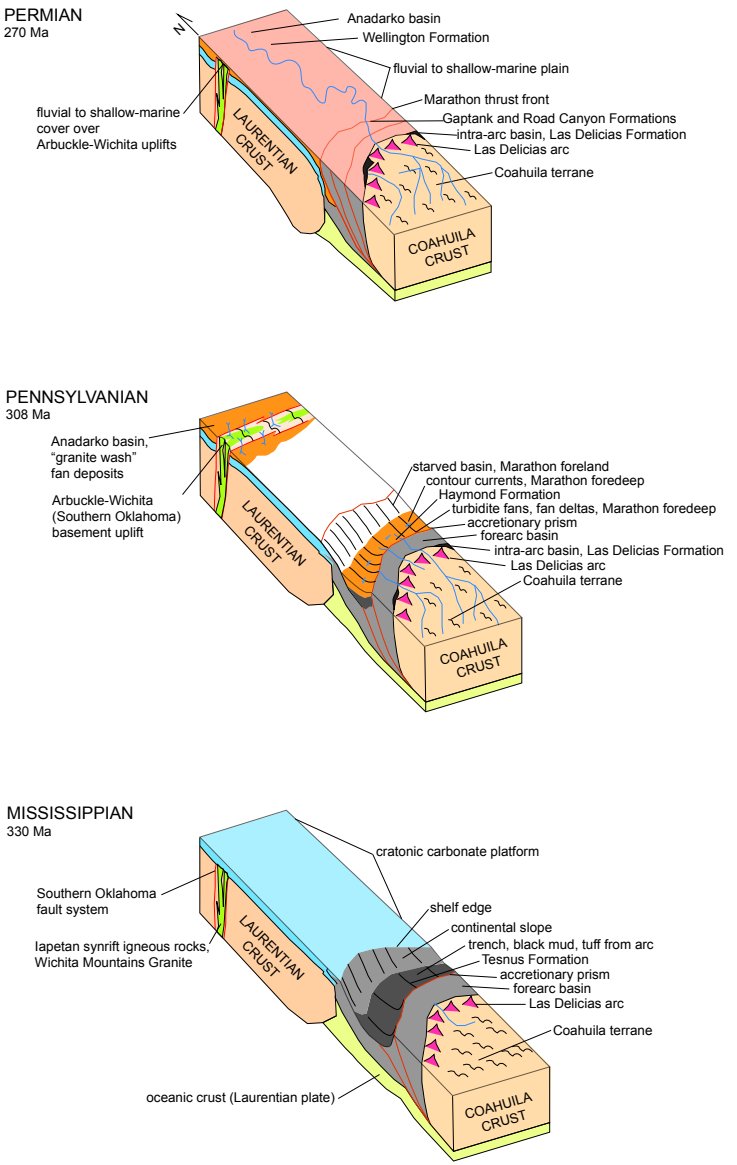

Figure 15. Sequence of three schematic block diagrams (not to scale), illustrating the interpreted dispersal pathways of detritus from the Coahuila terrane into the Marathon foreland and onto the southern craton of Laurentia, in the context of the tectonic evolution of the Marathon orogen and accretion of the Coahuila terrane to the southern margin of Laurentia. Long direction of the blocks is approximately north-south. See text for further discussion.

of some volcanic rocks in Las Delicias arc in Coahuila, suggesting that the arc was the source of the ash. The Pennsylvanian Haymond Formation consists of turbidites that represent downslope fan deposits, as well as contour currents (Fig. 15). The thick succession of turbidites evidently was restricted to a relatively narrow foredeep, which was bordered by a starved basin on the adjacent Laurentian shelf (Fig. 15). The Upper Pennsylvanian Gaptank and Middle Permian Road Canyon Formations consist of interbedded thin units of siliciclastic rocks and limestone; carbonate grains in the sandstones indicate local reworking on a low-relief plain. These units effectively cover the Marathon thrust front and distal foreland (Fig. 15). The detrital-zircon population of the Permian Wellington Formation in the cover of the Arbuckle-Wichita uplifts indicates a source like that of the sandstones in the Marathon foreland and a long dispersal pathway across the southern craton of Laurentia from the Coahuila terrane (Fig. 15). The detrital-zircon populations of the sandstones in the Marathon foreland, as well as the distant southern craton, all document a source in the Coahuila terrane.

ACKNOWLEDGMENTS

Sample collecting in Texas and analyses were funded by National Science Foundation (NSF) award EAR-1304980 to Gehrels and Thomas. Satterfield acknowledges logistical assistance and access to ranches from Gordon Buescher, Conoly Brooks III, and Beverly and John Landgraf. Leslie Williams, an undergraduate student at Angelo State University, assisted Satterfield in the collection of samples from the Marathon foreland and also conducted point-counting of sample TX-14-PGT. Lawton thanks Roberto Molina-Garza for assistance in collecting samples at Potrero Colorado in Mexico and gratefully acknowledges James McKee for enlightening discussions of Coahuila block geology. U-Pb analyses of Jurassic and Cretaceous samples from Mexico were funded by a Fulbright–Garcia Robles Research Fellowship to Lawton. All analyses were conducted at the Arizona LaserChron Center with the support of NSF awards EAR-0732436 and EAR-1338583. Ed Osborne and Phil Frederick provided helpful reviews of a preliminary draft of the manuscript. We acknowledge useful reviews by the *Geosphere* associate editor and reviewers Ryan Leary and Bob Stern.

REFERENCES CITED

Alsalem, O.B., Fan, M., Zamora, J., Xie, X., and Griffin, W.R., 2018, Paleozoic sediment dispersal before and during the collision between Laurentia and Gondwana in the Fort Worth basin, USA: Geosphere, v. 14, p. 325–342, https://doi.org/10.1130/GES01480.1.

Arbenz, J.K., 1989, The Ouachita system, *in* Bally, A.W., and Palmer, A.R., eds., The Geology of North America—An Overview: Boulder, Colorado, Geological Society of America, The Geology of North America, v. A, p. 371–396, https://doi.org/10.1130/DNAG-GNA-A.371.

Bickford, M.E., Mueller, P.A., Kamenov, G.D., and Hill, B.M., 2008, Crustal evolution of southern Laurentia during the Paleoproterozoic: Insights from zircon Hf isotopic studies of ca. 1.75 Ga rocks in central Colorado: Geology, v. 36, p. 555–558, https://doi.org/10.1130/G24700A.1.

Bickford, M.E., McLelland, J.M., Mueller, P.A., Kamenov, G.D., and Neadle, M., 2010, Hafnium isotopic compositions of zircon from Adirondack AMCG suites: Implications for the petrogenesis of anorthosites, gabbros, and granitic members of the suites: Canadian Mineralogist, v. 48, p. 751–761, https://doi.org/10.3749/canmin.48.2.751.

Bouvier, A., Vervoort, J.D., and Patchett, J.D., 2008, The Lu-Hf and Sm-Nd isotopic composition of CHUR: Constraints from unequilibrated chondrites and implications for the bulk composition of terrestrial planets: Earth and Planetary Science Letters, v. 273, p. 48–57, https://doi.org/10.1016/j.epsl.2008.06.010.

Brown, L.F., Jr., 1973, Pennsylvanian rocks of north-central Texas: An introduction, *in* Brown, L.F., Jr., Cleaves, A.W., II, and Erxleben, A.W., eds., Pennsylvanian Depositional Systems in North-Central Texas: Texas Bureau of Economic Geology Guidebook 14, p. 1–7.

Cameron, K.L., López, R., Ortega-Gutiérrez, F., Solari, L.A., Keppie, J.D., and Schulze, C., 2004, U-Pb geochronology and Pb isotope compositions of leached feldspars: Constraints on the origin and evolution of Grenvillian rocks from eastern and southern Mexico, *in* Tollo, R.P., Corriveau, L., McLelland, J., and Bartholomew, M.J., eds., Proterozoic Tectonic Evolution of the Grenville Orogen in North America: Geological Society of America Memoir 197, p. 755–769, https://doi.org/10.1130/0-8137-1197-5.755.

Campa, M.F., and Coney, P.J., 1983, Tectono-stratigraphic terranes and mineral resource distributions of Mexico: Canadian Journal of Earth Sciences, v. 20, p. 1040–1051, https://doi.org/10.1139/e83-094.

Cardona, A., Chew, D., Valencia, V.A., Bayona, G., Miskovic, A., and Ibañez-Mejía, M., 2010, Grenvillian remnants in the Northern Andes: Rodinian and Phanerozoic paleogeographic perspectives: Journal of South American Earth Sciences, v. 29, p. 92–104, https://doi.org/10.1016/j.jsames.2009.07.011.

Cecil, R., Gehrels, G., Patchett, J., and Ducea, M., 2011, U-Pb-Hf characterization of the central Coast Mountains batholith: Implications for petrogenesis and crustal architecture: Lithosphere, v. 3, p. 247–260, https://doi.org/10.1130/L134.1.

Centeno-García, E., 2005, Review of Upper Paleozoic and Lower Mesozoic stratigraphy and depositional environments of central and west Mexico: Constraints on terrane analysis and paleogeography, *in* Anderson, T.H., Nourse, J.A., McKee, J.W., and Steiner, M.B., eds., The Mojave-Sonora Megashear Hypothesis: Development, Assessment, and Alternatives: Geological Society of America Special Paper 393, p. 233–258, https://doi.org/10.1130/0-8137-2393-0.233.

Charleston, S., 1981, A summary of the structural geology and tectonics of the state of Coahuila, Mexico, *in* Smith, C.I., and Katzs, S.B., eds., Lower Cretaceous Stratigraphy and Structure, Northern Mexico: West Texas Geological Society Publication 81–74, p. 28–36.

Chávez-Cabello, G., Aranda-Gomez, J.J., Molina-Garza, R.S., Cossio-Torres, T., Arvizu-Gutiérrez, I.R., and González-Naranjo, G.A., 2005, La falla San Marcos: Una estructura jurásica de basamento multirreactivada del noreste de México: Boletín de la Asociacion Geológica Mexicana, v. 17, p. 27–52.

Cohen, K.M., Finney, S.C., Gibbard, P.L., and Fan, J.-X., 2013, updated, The ICS International Chronostratigraphic Chart: Episodes, v. 36, p. 199–204.

Cordani, U.G., and Teixeira, W., 2007, Proterozoic accretionary belts in the Amazonian craton, *in* Hatcher, R.D., Jr., Carlson, M.P., McBride, J.H., and Martínez Catalán, J.R., eds., 4-D Framework of Continental Crust: Geological Society of America Memoir 200, p. 297–320, https://doi.org/10.1130/2007.1200(14).

Cordani, U.G., Sato, K., Teixeira, W., Tassinari, C.C.G., and Basei, M.A.S., 2000, Crustal evolution of the South American platform, *in* Cordani, U.G., Milani, E.J., Thomaz-Filho, A., and Campos, D.A., eds., Tectonic Evolution of South America: 31st International Geological Congress: Rio de Janeiro, Brazil, p. 19–40.

Cristofolini, E.A., Otamendi, J.E., Ducea, M.N., Pearson, D.M., Tibaldi, A.M., and Baliani, I., 2012, Detrital zircon U/Pb ages of metasedimentary rocks from Sierra de Valle Fértil: Entrapment of middle and late Cambrian marine successions in the deep roots of the Early Ordovician Famatinian arc: Journal of South American Earth Sciences, v. 37, p. 77–94, https://doi.org/10.1016/j.jsames.2012.02.001.

Denison, R.E., Kenny, G.S., Burke, W.H., Jr., and Hetherington, E.A., Jr., 1969, Isotopic ages of igneous and metamorphic boulders from the Haymond Formation (Pennsylvanian), Marathon Basin, Texas, and their significance: Geological Society of America Bulletin, v. 80, p. 245–256, https://doi.org/10.1130/0016-7606(1969)80[245:IAOIAM]2.0.CO;2.

Denison, R.E., Housh, T.B., and McDowell, F.W., 2005, New ages from the crystalline Haymond boulders, Marathon Basin, Texas: Geological Society of America Abstracts with Programs, v. 37, no. 2, p. 38.

Dickinson, W.R., 1985, Interpreting provenance from detrital modes of sandstones, *in* Zuffa, G.G., ed., Provenance of Arenites: Dordrecht, Netherlands, D. Reidel, p. 333–361, https://doi.org/10.1007/978-94-017-2809-6_15.

Dickinson, W.R., and Lawton, T.F., 2001, Carboniferous to Cretaceous assembly and fragmentation of Mexico: Geological Society of America Bulletin, v. 113, p. 1142–1160, https://doi.org/10.1130/0016-7606(2001)113<1142:CTCAAF>2.0.CO;2.

Dickinson, W.R., Gehrels, G.E., and Stern, R.J., 2010, Late Triassic Texas uplift preceding Jurassic opening of the Gulf of Mexico: Evidence from U-Pb ages of detrital zircons: Geosphere, v. 6, p. 641–662, https://doi.org/10.1130/GES00532.1.

Dirección General de Geografía del Territorio Nacional, 1980a, Carta Geologica—Chihuahua: Mexico, D.F., Secretaría de Programación y Presupuesto, Coordinación General de los Servicios Nacionales de Estadistica, Geografía e Informatica, 1 sheet, scale 1:1,000,000.

Dirección General de Geografía del Territorio Nacional, 1980b, Carta Geologica—Monterrey: Mexico, D.F., Secretaría de Programación y Presupuesto, Coordinación General de los Servicios Nacionales de Estadistica, Geografía e Informatica, 1 sheet, scale 1:1,000,000.

Dirección General de Geografía del Territorio Nacional, 1982, Carta Estatal Geologica—Estado de Coahuila: Mexico, D.F.: Secretaría de Programación y Presupuesto, Coordinación General de los Servicios Nacionales de Estadistica, Geografía e Informatica, 1 sheet, scale 1:1,000,000.

Eguiluz de Antuñano, S., 1989, La formacion Carbonera y sus implicaciones tectonicas, estados de Coahuila y Nuevo Leon: Boletín de la Sociedad Geológica Mexicana, v. 50, p. 3–39, https://doi.org/10.18268/BSGM1989v50n1a1.

Eguiluz de Antuñano, S., 2001, Geologic evolution and gas resources of the Sabinas basin in northeastern Mexico, *in* Bartolini, C., Buffler, R.T., and Cantú-Chapa, A., eds., The Western Gulf of Mexico Basin: American Association of Petroleum Geologists Memoir 75, p. 241–270.

Eguiluz de Antuñano, S., Aranda-Garcia, M., and Marrett, R., 2000, Tectónica de la Sierra Madre Oriental, México: Boletín de la Sociedad Geológica Mexicana, v. 53, p. 1–26, https://doi.org/10.18268/BSGM2000v53n1a1.

Ethington, R.L., Finney, S.C., and Repetski, J.E., 1989, Biostratigraphy of the Paleozoic rocks of the Ouachita orogen, Arkansas, Oklahoma, west Texas, *in* Hatcher, R.D., Jr., Thomas, W.A., and Viele, G.W., eds., The Appalachian-Ouachita Orogen in the United States: Boulder, Colorado, Geological Society of America, The Geology of North America, v. F-2, p. 563–574, https://doi.org/10.1130/DNAG-GNA-F2.563.

Fitz-Díaz, E., Lawton, T.F., Juárez-Arriaga, E., and Chávez-Cabello, G., 2018, The Cretaceous–Paleogene Mexican orogen: Structure, basin development, magmatism and tectonics: Earth-Science Reviews, v. 183, p. 56–84, https://doi.org/10.1016/j.earscirev.2017.1003.1002.

Fortunato, K.S., and Ward, W.C., 1982, Upper Jurassic–Lower Cretaceous fan-delta complex, La Casita Formation of the Saltillo area, Coahuila, Mexico: Gulf Coast Association of Geological Societies Transactions, v. 32, p. 473–482.

Garzanti, E., 2016, From static to dynamic provenance analysis—Sedimentary petrology upgraded: Sedimentary Geology, v. 336, p. 3–13, https://doi.org/10.1016/j.sedgeo.2015.07.010.

Gehrels, G.E., 2000, Introduction to detrital zircon studies of Paleozoic and Triassic strata in western Nevada and northern California, *in* Soreghan, M.J., and Gehrels, G.E., eds., Paleozoic and Triassic Paleogeography and Tectonics of Western Nevada and Northern California: Geological Society of America Special Paper 347, p. 1–17, https://doi.org/10.1130/0-8137-2347-7.1.

Gehrels, G.E., and Pecha, M.E., 2014, Detrital zircon U-Pb geochronology and Hf isotope geochemistry of Paleozoic and Triassic passive margin strata of western North America: Geosphere, v. 10, p. 49–65, https://doi.org/10.1130/GES00889.1.

Gehrels, G.E., Valencia, V., and Ruiz, J., 2008, Enhanced precision, accuracy, efficiency, and spatial resolution of U-Pb ages by laser ablation–multicollector–inductively coupled plasma–mass spectrometry: Geochemistry Geophysics Geosystems, v. 9, Q03017, https://doi.org/10.1029/2007GC001805.

Gleason, J.D., Patchett, P.J., Dickinson, W.R., and Ruiz, J., 1994, Nd isotopes link Ouachita turbidites to Appalachian sources: Geology, v. 22, p. 347–350, https://doi.org/10.1130/0091-7613(1994)022<0347:NILOTT>2.3.CO;2.

Gleason, J.D., Gehrels, G.E., Dickinson, W.R., Patchett, P.J., and Kring, D.A., 2007, Sources of detrital zircon grains in turbidite and deltaic sandstones of the Lower to Middle Pennsylvanian Haymond Formation, Marathon assemblage, Texas: Journal of Sedimentary Research, v. 77, p. 888–900, https://doi.org/10.2110/jsr.2007.084.

González-Naranjo, G.A., Molina-Garza, R.S., and Chávez-Cabello, G., 2008, Paleomagnetic study of Jurassic and Cretaceous rocks north of San Marcos fault, central Coahuila, México: Geofísica Internacional, v. 47, p. 41–55.

Goodge, J.W., and Vervoort, J.D., 2006, Origin of Mesoproterozoic A-type granites in Laurentia: Hf isotope evidence: Earth and Planetary Science Letters, v. 243, p. 711–731, https://doi.org/10.1016/j.epsl.2006.01.040.

Graham, S.A., Ingersoll, R.V., and Dickinson, W.R., 1976, Common provenance for lithic grains in Carboniferous sandstones from Ouachita Mountains and Black Warrior Basin: Journal of Sedimentary Petrology, v. 46, p. 620–632, https://doi.org/10.1306/212F7009-2B24-11D7-8648000102C1865D.

Gray, G.G., Lawton, T.F., and Murphy, J.J., 2008, Looking for the Mojave-Sonora megashear in northeastern Mexico, *in* Moore, G., ed., Geological Society of America Field Guide, 2008 Joint Annual Meeting, Houston, Texas, 5–9 October 2008: Geological Society of America Field Guide 14, p. 1–25, https://doi.org/10.1130/2008.fld014(01).

Hamlin, H.S., 2009, Ozona sandstone, Val Verde Basin, Texas: Synorogenic stratigraphy and depositional history in a Permian foredeep basin: American Association of Petroleum Geologists Bulletin, v. 93, p. 573–594, https://doi.org/10.1306/01200908121.

Hatcher, R.D., Jr., 2010, The Appalachian orogen: A brief summary, *in* Tollo, R.P., Bartholomew, M.J., Hibbard, J.P., and Karabinos, P.M., eds., From Rodinia to Pangea: The Lithotectonic Record of the Appalachian Region: Geological Society of America Memoir 206, p. 1–19, https://doi.org/10.1130/2010.1206(01).

Henderson, B.J., Collins, W.J., Murphy, J.B., Gutierrez-Alonso, G., and Hand, M., 2015, Gondwanan basement terranes of the Variscan-Appalachian orogen: Baltican, Saharan and West African hafnium isotopic fingerprints in Avalonia, Iberia and the Armorican terranes: Tectonophysics, v. 681, p. 278–304, https://doi.org/10.1016/j.tecto.2015.11.020.

Hibbard, J.P., van Staal, C.R., and Miller, B.V., 2007, Links among Carolinia, Avalonia, and Ganderia in the Appalachian peri-Gondwanan realm, *in* Sears, J.W., Harms, T.A., and Evenchick, C.A., eds., Whence the Mountains? Inquiries into the Evolution of Orogenic Systems: A Volume in Honor of Raymond A. Price: Geological Society of America Special Paper 433, p. 291–311, https://doi.org/10.1130/2007.2433(14).

Hickman, R.C., Varga, R.J., and Altany, R.M., 2009, Structural style of the Marathon thrust belt, west Texas: Journal of Structural Geology, v. 31, p. 900–909, https://doi.org/10.1016/j.jsg.2008.02.016.

Humphrey, W.E., and Díaz, T., 2003, Jurassic and Lower Cretaceous Stratigraphy and Tectonics of Northeast Mexico: Austin, Texas, Bureau of Economic Geology, Report of Investigations 267, 152 p.

Imoto, N., and McBride, E.F., 1990, Volcanism recorded in Tesnus Formation, Marathon uplift, Texas, *in* Laroche, T.M., and Higgins, L., eds., Marathon Thrust Belt: Structure, Stratigraphy, and Hydrocarbon Potential: 1990 Field Seminar: West Texas Geological Society, Permian Basin Section, Society of Economic Paleontologists and Mineralogists (SEPM), p. 93–98.

Ingersoll, R.V., Bullard, T.F., Ford, R.L., Grimm, J.P., Pickle, J.D., and Sares, S.W., 1984, The effect of grain size on detrital modes: A test of the Gazzi-Dickinson point-counting method: Journal of Sedimentary Petrology, v. 54, p. 103–116.

Jansen, X., 2014, Early to Mid-Permian Stratigraphy and Slope System in the Southern Delaware Basin, Glass Mountains: Midland, Texas, Southwest Section, American Association of Petroleum Geologists, Field Trip May 8–11, 2014, 82 p.

Johnson, K.S., Amsden, T.W., Denison, R.E., Dutton, S.P., Goldstein, A.G., Rascoe, B., Jr., Sutherland, P.K., and Thompson, D.M., 1988, Southern Midcontinent region, *in* Sloss, L.L., ed., Sedimentary Cover—North American Craton: U.S.: Boulder, Colorado, Geological Society of America, The Geology of North America, v. D-2, p. 307–359, https://doi.org/10.1130/DNAG-GNA-D2.307.

Jones, N.W., McKee, J.W., Marquez, D.B., Tovar, J., Long, L.E., and Laudon, T.S., 1984, The Mesozoic La Mula island, Coahuila, Mexico: Geological Society of America Bulletin, v. 95, p. 1226–1241, https://doi.org/10.1130/0016-7606(1984)95<1226:TMLMIC>2.0.CO;2.

Keller, G.R., Kruger, J.M., Smith, K.J., and Voight, W.M., 1989a, The Ouachita system; a geophysical overview, *in* Hatcher, R.D., Jr., Thomas, W.A., and Viele, G.W., eds., The Appalachian-Ouachita Orogen in the United States: Boulder, Colorado, Geological Society of America, The Geology of North America, v. F-2, p. 689–694, https://doi.org/10.1130/DNAG-GNA-F2.689.

Keller, G.R., Braile, L.W., McMechan, G.A., Thomas, W.A., Harder, S.H., Chang, W.-F., and Jardine, W.G., 1989b, Paleozoic continent-ocean transition in the Ouachita Mountains imaged from PASSCAL wide-angle seismic reflection-refraction data: Geology, v. 17, p. 119–122, https://doi.org/10.1130/0091-7613(1989)017<0119:PCOTIT>2.3.CO;2.

King, P.B., 1930, Geology of the Glass Mountains: Part 1. Descriptive Geology: Austin, Texas, University of Texas, Bureau of Economic Geology Bulletin 3038, 167 p.

King, P.B., 1937, Geology of the Marathon Region, Texas: U.S. Geological Survey Professional Paper 187, 148 p.

King, P.B., 1980, Geology of the Eastern Part of the Marathon Basin, Texas: U.S. Geological Survey Professional Paper 1157, 40 p., https://doi.org/10.3133/pp1157.

Krogh, T.E., Kamo, S.L., Sharpton, V.L., Marin, L.E., and Hildebrand, A.R., 1993, U-Pb ages of single shocked zircons linking distal K/T ejecta to the Chicxulub crater: Nature, v. 366, p. 731–734, https://doi.org/10.1038/366731a0.

Krutak, P.R., 1965, Source areas of the Patula Arkose (Lower Cretaceous), Coahuila, Mexico: Journal of Sedimentary Petrology, v. 35, p. 512–518, https://doi.org/10.1306/74D712E4-2B21-11D7-8648000102C1865D.

Lawlor, P.J., Ortega-Gutierrez, F., Cameron, K.L., Ochoa-Camarillo, H., Lopez, R., and Sampson, D.E., 1999, U-Pb geochronology, geochemistry, and provenance of the Grenvillian Huiznopala Gneiss of eastern Mexico: Precambrian Research, v. 94, p. 73–99, https://doi.org/10.1016/S0301-9268(98)00108-9.

Lawton, T.F., and Molina-Garza, R.S., 2014, U-Pb geochronology of the type Nazas Formation and superjacent strata, northeastern Durango, Mexico: Implications of a Jurassic age for continental-arc magmatism in north-central Mexico: Geological Society of America Bulletin, v. 126, p. 1181–1199, https://doi.org/10.1130/B30827.1.

Lopez, R., 1997, High-Mg Andesites from the Gila Bend Mountains, Southwestern Arizona: Evidence for Hydrous Melting of Lithosphere during Miocene Extension; *and* The Pre-Jurassic Geotectonic Evolution of the Coahuila Terrane, Northwestern Mexico: Grenville Basement, a Late Paleozoic Arc, Triassic Plutonism, and the Events South of the Ouachita Suture [Ph.D. thesis]: Santa Cruz, California, University of California–Santa Cruz, 147 p.

Lopez, R., Cameron, K.L., and Jones, N.W., 2001, Evidence for Paleoproterozoic, Grenvillian, and Pan-African age Gondwanan crust beneath northeastern Mexico: Precambrian Research, v. 107, p. 195–214, https://doi.org/10.1016/S0301-9268(00)00140-6.

Martens, U., Weber, B., and Valencia, V.A., 2010, U/Pb geochronology of Devonian and older Paleozoic beds in the southeastern Maya block, Central America: Its affinity with peri-Gondwanan terranes: Geological Society of America Bulletin, v. 122, p. 815–829, https://doi.org/10.1130/B26405.26401.

McBride, E.F., 1964, Stratigraphy and sedimentology of the Gaptank Formation, Marathon Basin, Texas, *in* Thompson, A., ed., The Filling of the Marathon Geosyncline, Symposium and Guidebook: Permian Basin Section, Society of Economic Paleontologists and Mineralogists (SEPM) Publication 64–9, p. 41–44.

McBride, E.F., 1989, Stratigraphy and sedimentary history of pre-Permian Paleozoic rocks of the Marathon uplift, *in* Hatcher, R.D., Jr., Thomas, W.A., and Viele, G.W., eds., The Appalachian-Ouachita Orogen in the United States: Boulder, Colorado, Geological Society of America, The Geology of North America, v. F-2, p. 603–620, https://doi.org/10.1130/DNAG-GNA-F2.603.

McKee, J.W., Jones, N.W., and Long, L.E., 1984, History of recurrent activity along a major fault in northeastern Mexico: Geology, v. 12, p. 103–107, https://doi.org/10.1130/0091-7613(1984)12<103:HORAAA>2.0.CO;2.

McKee, J.W., Jones, N.W., and Anderson, T.H., 1988, Las Delicias basin: A record of late Paleozoic arc volcanism in northeastern Mexico: Geology, v. 16, p. 37–40, https://doi.org/10.1130/0091-7613(1988)016<0037:LDBARO>2.3.CO;2.

McKee, J.W., Jones, N.W., and Long, L.E., 1990, Stratigraphy and provenance of strata along the San Marcos fault, central Coahuila, Mexico: Geological Society of America Bulletin, v. 102, p. 593–614, https://doi.org/10.1130/0016-7606(1990)102<0593:SAPOSA>2.3.CO;2.

McKee, J.W., Jones, N.W., and Anderson, T.H., 1999, The late Paleozoic and early Mesozoic history of the Las Delicias terrane, Coahuila, Mexico, *in* Bartolini, C., Wilson, J.L., and Lawton, T.F., eds., Mesozoic Sedimentary and Tectonic History of North Central Mexico: Geological Society of America Special Paper 340, p. 161–189, https://doi.org/10.1130/0-8137-2340-X.161.

Mickus, K.L., and Keller, G.R., 1992, Lithospheric structure of the south-central United States: Geology, v. 20, p. 335–338, https://doi.org/10.1130/0091-7613(1992)020<0335:LSOTSC>2.3.CO;2.

Muehlberger, W.R., and Tauvers, P.R., 1989, Marathon fold-thrust belt, west Texas, *in* Hatcher, R.D., Jr., Thomas, W.A., and Viele, G.W., eds., The Appalachian-Ouachita Orogen in the United States: Boulder, Colorado, Geological Society of America, The Geology of North America, v. F-2, p. 673–680, https://doi.org/10.1130/DNAG-GNA-F2.673.

Mueller, P., Foster, D., Mogk, D., Wooden, J., and Vogl, J., 2007, Detrital mineral chronology of the Uinta Mountain Group: Implications of the Grenville flood in southwestern Laurentia: Geology, v. 35, p. 431–434, https://doi.org/10.1130/G23148A.1.

Mueller, P.A., Kamenov, G.D., Heatherington, A.L., and Richards, J., 2008, Crustal evolution in the southern Appalachian orogen: Evidence from Hf isotopes in detrital zircons: The Journal of Geology, v. 116, p. 414–422, https://doi.org/10.1086/589311.

Ocampo-Díaz, Y.Z.E., Talavera-Mendoza, O., Jenchen, U., Valencia, V.A., Medina-Ferrusquia, H.C., and Guerrero-Suastegui, M., 2014, Procedencia de la Formación La Casita y la Arcosa Patula: Implicaciones para la evolución tectono-magmática del NE de México entre el Carbonífero y el Jurásico: Revista Mexicana de Ciencias Geológicas, v. 31, p. 45–63.

Ortega-Gutierrez, F., Ruiz, J., and Centeno-Garcia, E., 1995, Oaxaquia, a Proterozoic microcontinent accreted to North America during the late Paleozoic: Geology, v. 23, p. 1127–1130, https://doi.org/10.1130/0091-7613(1995)023<1127:OAPMAT>2.3.CO;2.

Palmer, A.R., DeMis, W.D., Muehlberger, W.R., and Robison, R.A., 1984, Geological implications of Middle Cambrian boulders from the Haymond Formation (Pennsylvanian) in the Marathon Basin, west Texas: Geology, v. 12, p. 91–94, https://doi.org/10.1130/0091-7613(1984)12<91:GIOMCB>2.0.CO;2.

Pepper, M., Gehrels, G., Pullen, A., Ibañez-Mejía, M., Ward, K.M., and Kapp, P., 2016, Magmatic history and crustal genesis of western South America: Constraints from U-Pb ages and Hf isotopes of detrital zircons in modern rivers: Geosphere, v. 12, p. 1532–1555, https://doi.org/10.1130/GES01315.1.

Pettijohn, F.J., Potter, P.E., and Siever, R., 1987, Sand and Sandstone: New York, Springer-Verlag, 218 p., https://doi.org/10.1007/978-1-4612-1066-5.

Pindell, J.L., and Kennan, L., 2009, Tectonic evolution of the Gulf of Mexico, Caribbean and northern South America in the mantle reference frame: An update, *in* James, K.H., Lorente, M.A., and Pindell, J.L., eds., The Origin and Evolution of the Caribbean Plate: Geological Society [London] Special Publication 328, p. 1–55, https://doi.org/10.1144/SP328.1.

Pollock, J.C., Sylvester, P.J., and Barr, S.M., 2015, Lu-Hf zircon and Sm-Nd whole-rock isotope constraints on the extent of juvenile arc crust in Avalonia: Examples from Newfoundland and Nova Scotia, Canada: Canadian Journal of Earth Sciences, v. 52, p. 161–181, https://doi.org/10.1139/cjes-2014-0157.

Poole, F.G., Perry, W.J., Jr., Madrid, R.J., and Amaya-Martínez, R., 2005, Tectonic synthesis of the Ouachita-Marathon-Sonora orogenic margin of southern Laurentia: Stratigraphic and structural implications for timing of deformational events and plate-tectonic model, *in* Anderson, T.H., Nourse, J.A., McKee, J.W., and Steiner, M.B., eds., The Mohave-Sonora Megashear Hypothesis: Development, Assessment, and Alternatives: Geological Society of America Special Paper 393, p. 543–596, https://doi.org/10.1130/0-8137-2393-0.543.

Ross, C.A., 1967, Stratigraphy and depositional history of the Gaptank Formation (Pennsylvanian), west Texas: Geological Society of America Bulletin, v. 78, p. 369–384, https://doi.org/10.1130/0016-7606(1967)78[369:SADHOT]2.0.CO;2.

Ross, C.A., 1986, Paleozoic evolution of southern margin of Permian basin: Geological Society of America Bulletin, v. 97, p. 536–554, https://doi.org/10.1130/0016-7606(1986)97<536:PEOSMO>2.0.CO;2.

Sedlock, R.L., Ortega-Gutierrez, F., and Speed, R.C., 1993, Tectonostratigraphic Terranes and Tectonic Evolution of Mexico: Geological Society of America Special Paper 278, 153 p., https://doi.org/10.1130/SPE278-p1.

Servicio Geológico Mexicano, 2005, Carta Magnética de la República Mexicana (scale 1:4,000,000): https://mapserver.sgm.gob.mx/Cartas_Online/geofisica/carta_magnetica_republica.pdf (accessed 29 May 2018).

Silverman, B.W., 1986, Density Estimation for Statistics and Data Analysis: London, Chapman and Hall, 175 p., https://doi.org/10.1007/978-1-4899-3324-9.

Smith, C.I., 1981, Review of the geologic setting, stratigraphy, and facies distribution of the Lower Cretaceous in northern Mexico, *in* Katz, S.B., and Smith, C.I., eds., Lower Cretaceous Stratigraphy and Structure, Northern Mexico: West Texas Geological Society Publication 81–74, p. 1–27.

Soreghan, G.S., and Soreghan, M.J., 2013, Tracing clastic delivery to the Permian Delaware basin, U.S.A.: Implications for paleogeography and circulation in westernmost equatorial Pangea: Journal of Sedimentary Research, v. 83, p. 786–802, https://doi.org/10.2110/jsr.2013.63.

Steiner, M.B., and Walker, J.D., 1996, Late Silurian plutons in Yucatan: Journal of Geophysical Research, v. 101, p. 17,727–17,735, https://doi.org/10.1029/96JB00174.

Stewart, J.H., Blodgett, R.B., Boucot, A.J., Carter, J.L., and Lopez, R., 1999, Exotic Paleozoic strata of Gondwanan provenance near Ciudad Victoria, Tamaulipas, Mexico, *in* Ramos, V.A., and Keppie, J.D., eds., Laurentia–Gondwana Connections before Pangea: Geological Society of America Special Paper 336, p. 227–252, https://doi.org/10.1130/0-8137-2336-1.227.

Tassinari, C.C.G., Bettencourt, J.S., Geraldes, M.C., Macambira, M.J.B., and Lafon, J.M., 2000, The Amazon craton, *in* Cordani, U.G., Milani, E.J., Thomaz-Filho, A., and Campos, D.A., eds., Tectonic Evolution of South America: 31st International Geological Congress: Rio de Janeiro, Brazil, p. 19–40.

Thomas, W.A., 1977, Evolution of Appalachian-Ouachita salients and recesses from reentrants and promontories in the continental margin: American Journal of Science, v. 277, p. 1233–1278, https://doi.org/10.2475/ajs.277.10.1233.

Thomas, W.A., 2006, Tectonic inheritance at a continental margin [2005 Geological Society of America Presidential Address]: GSA Today, v. 16, no. 2, p. 4–11, https://doi.org/10.1130/1052-5173(2006)016[4:TIAACM]2.0.CO;2.

Thomas, W.A., 2014, A mechanism for tectonic inheritance at transform faults of the Iapetan margin of Laurentia: Geoscience Canada, v. 41, p. 321–344, https://doi.org/10.12789/geocanj.2014.41.048.

Thomas, W.A., Viele, G.W., Arbenz, J.K., Nicholas, R.L., Denison, R.E., Muehlberger, W.R., and Tauvers, P.R., 1989, Tectonic map of the Ouachita orogen, *in* Hatcher, R.D., Jr., Thomas, W.A., and Viele, G.W., eds., The Appalachian-Ouachita Orogen in the United States: Boulder, Colorado, Geological Society of America, The Geology of North America, v. F-2, Plate 9.

Thomas, W.A., Gehrels, G.E., and Romero, M.C., 2016, Detrital zircons from crystalline rocks along the Southern Oklahoma fault system, Wichita and Arbuckle Mountains, USA: Geosphere, v. 12, p. 1224–1234, https://doi.org/10.1130/GES01316.1.

Thomas, W.A., Gehrels, G.E., Greb, S.F., Nadon, G.C., Satkoski, A.M., and Romero, M.C., 2017, Detrital zircons and sediment dispersal in the Appalachian foreland: Geosphere, v. 13, p. 2206–2230, https://doi.org/10.1130/GES01525.1.

Van Schmus, W.R., Bickford, M.E., Anderson, J.L., Bender, E.E., Anderson, R.R., Bauer, P.W., Robertson, J.M., Bowring, S.A., Condie, K.C., Denison, R.E., Gilbert, M.C., Grambling, J.A., Mawer, C.K., Shearer, C.K., Hinze, W.J., Karlstrom, K.E., Kisvarsanyi, E.B., Lidiak, E.G., Reed, J.C., Jr., Sims, P.K., Tweto, O., Silver, L.T., Treves, S.B., Williams, M.L., and Wooden, J.L., 1993, Transcontinental Proterozoic provinces, *in* Reed, J.C., Jr., Bickford, M.E., Houston, R.S., Link, P.K., Rankin, D.W., Sims, P.K., and Van Schmus, W.R., eds., Precambrian: Conterminous U.S.: Boulder, Colorado, Geological Society of America, The Geology of North America, v. C-2, p. 171–334, https://doi.org/10.1130/DNAG-GNA-C2.171.

Vervoort, J.D., and Patchett, P.J., 1996, Behavior of hafnium and neodymium isotopes in the crust: Constraints from crustally derived granites: Geochimica et Cosmochimica Acta, v. 60, no. 19, p. 3717–3733, https://doi.org/10.1016/0016-7037(96)00201-3.

Vervoort, J.D., Patchett, P.J., Blichert-Toft, J., and Albarede, F., 1999, Relationships between Lu-Hf and Sm-Nd isotopic systems in the global sedimentary system: Earth and Planetary Science Letters, v. 168, p. 79–99, https://doi.org/10.1016/S0012-821X(99)00047-3.

Viele, G.W., and Thomas, W.A., 1989, Tectonic synthesis of the Ouachita orogenic belt, *in* Hatcher, R.D., Jr., Thomas, W.A., and Viele, G.W., eds., The Appalachian-Ouachita Orogen in the United States: Boulder, Colorado, Geological Society of America, The Geology of North America, v. F-2, p. 695–728, https://doi.org/10.1130/DNAG-GNA-F2.695.

Willner, A.P., Barr, S.M., Gerdes, A., Massonne, H.-J., and White, C.E., 2013, Origin and evolution of Avalonia: Evidence from U-Pb and Lu-Hf isotopes in zircon from the Mira terrane, Canada, and the Stavelot–Venn Massif, Belgium: Journal of the Geological Society [London], v. 170, p. 769–784, https://doi.org/10.1144/jgs2012-152.

Willner, A.P., Gerdes, A., Massonne, H.-J., van Staal, C.R., and Zagorevski, A., 2014, Crustal evolution of the northeast Laurentian margin and the peri-Gondwanan microcontinent Ganderia prior to and during closure of the Iapetus Ocean: Detrital zircon U-Pb and Hf isotope evidence from Newfoundland: Geoscience Canada, v. 41, p. 345–364, https://doi.org/10.12789/geocanj.2014.41.046.

Xie, X., Anthony, J.M., and Busbey, A.B., 2018, Provenance of Permian Delaware Mountain Group, central and southern Delaware basin, and implications of sediment dispersal pathway near the southwestern terminus of Pangea: International Geology Review, v. 61, no. 3, p. 361–380, https://doi.org/10.1080/00206814.2018.1425925.